Power Transmission Engineering®

DECEMBER 2024

ULTRASONIC ANALYSIS

REGAL REXNORD CONVEYOR TECHNOLOGY

SOLVE INDUSTRIAL MOTION GROUP

TECHNICAL

Control System Techniques (Part 2)

Acoustic Behavior of Gearboxes Using Neural Networks

powertransmission.com

Power Transmission Engineering is POWERED by The American Gear Manufacturers Association

Power Transmission Engineering®

DECEMBER 2024

Power Transmission Engineering is POWERED by The American Gear Manufacturers Association

FEATURE ARTICLES

22

TECHNICAL ARTICLES

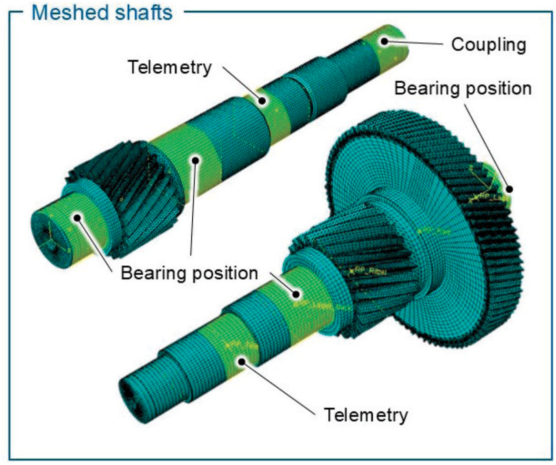

32

STAY CONNECTED

Connect with us on LinkedIn
linkedin.com/groups/Power-Transmission-Engineering-PTE-2950055

Subscribe Online
powertransmission.com/subscriptions

Vol. 18, No. 8. POWER TRANSMISSION ENGINEERING (ISSN 2331-2483) is published monthly except in January, May, July and November by The American Gear Manufacturers Association, 1001 N. Fairfax Street, Suite 500, Alexandria, VA 22314, (847) 437-6604.

Periodicals Postage Paid at Elk Grove Village IL and at additional mailing offices.

UNITED STATES POSTAL SERVICE®

Statement of Ownership, Management, and Circulation (Requester Publications Only)

1. Publication Title	2. Publication Number	3. Filing Date
POWER TRANSMISSION ENGINEERING	2331_2483	10/1/2024
4. Issue Frequency	**5. Number of Issues Published Annually**	**6. Annual Subscription Price** *(if any)*
Monthly except Jan., May, July, Nov.	8	

7. Complete Mailing Address of Known Office of Publication *(Not printer) (Street, city, county, state, and ZIP+4®)*
1840 JARVIS AVE., ELK GROVE VILLAGE, COOK COUNTY, IL 60007-2440

Contact Person

Telephone *(Include area code)*

8. Complete Mailing Address of Headquarters or General Business Office of Publisher *(Not printer)*
1840 JARVIS AVE., ELK GROVE VILLAGE, COOK COUNTY, IL 60007-2440

9. Full Names and Complete Mailing Addresses of Publisher, Editor, and Managing Editor *(Do not leave blank)*

Publisher *(Name and complete mailing address)* RANDY STOTT
1840 JARVIS AVE., ELK GROVE VILLAGE, COOK COUNTY, IL 60007-2440

Editor *(Name and complete mailing address)* RANDY STOTT
1840 JARVIS AVE., ELK GROVE VILLAGE, COOK COUNTY, IL 60007-2440

Managing Editor *(Name and complete mailing address)* RANDY STOTT
1840 JARVIS AVE., ELK GROVE VILLAGE, COOK COUNTY, IL 60007-2440

10. Owner *(Do not leave blank. If the publication is owned by a corporation, give the name and address of the corporation immediately followed by the names and addresses of all stockholders owning or holding 1 percent or more of the total amount of stock. If not owned by a corporation, give the names and addresses of the individual owners. If owned by a partnership or other unincorporated firm, give its name and address as well as those of each individual owner. If the publication is published by a nonprofit organization, give its name and address.)*

Full Name	Complete Mailing Address
AMERICAN GEAR MANUFACTURERS ASSOCIATION	1001 N. FAIRFAX ST., SUITE #500 ALEXANDRIA, VA 22314

11. Known Bondholders, Mortgagees, and Other Security Holders Owning or Holding 1 Percent or More of Total Amount of Bonds, Mortgages, or Other Securities. If none, check box. → ☒ None

Full Name	Complete Mailing Address

12. Tax Status *(For completion by nonprofit organizations authorized to mail at nonprofit rates) (Check one)*
The purpose, function, and nonprofit status of this organization and the exempt status for federal income tax purposes:
☐ Has Not Changed During Preceding 12 Months
☐ Has Changed During Preceding 12 Months *(Publisher must submit explanation of change with this statement.)*

PS Form **3526-R,** July 2014 *[Page 1 of 4 (See instructions page 4)]* PSN: 7530-09-000-8855 **PRIVACY NOTICE:** See our privacy policy on *www.usps.com.*

13. Publication Title: POWER TRANSMISSION ENGINEERING

14. Issue Date for Circulation Data Below: SEPTEMBER 2024

15. Extent and Nature of Circulation			Average No. Copies Each Issue During Preceding 12 Months	No. Copies of Single Issue Published Nearest to Filing Date
a. Total Number of Copies *(Net press run)*			12,745	13,020
b. Legitimate Paid and/or Requested Distribution *(By mail and outside the mail)*	(1)	Outside County Paid/Requested Mail Subscriptions stated on PS Form 3541. *(Include direct written request from recipient, telemarketing, and Internet requests from recipient, paid subscriptions including nominal rate subscriptions, employer requests, advertiser's proof copies, and exchange copies.)*	4,270	4,460
	(2)	In-County Paid/Requested Mail Subscriptions stated on PS Form 3541. *(Include direct written request from recipient, telemarketing, and Internet requests from recipient, paid subscriptions including nominal rate subscriptions, employer requests, advertiser's proof copies, and exchange copies.)*	-	-
	(3)	Sales Through Dealers and Carriers, Street Vendors, Counter Sales, and Other Paid or Requested Distribution Outside USPS®	211	150
	(4)	Requested Copies Distributed by Other Mail Classes Through the USPS (e.g., First-Class Mail®)	-	-
c. Total Paid and/or Requested Circulation *(Sum of 15b (1), (2), (3), and (4))* ▶			4,481	4,610
d. Non-requested Distribution *(By mail and outside the mail)*	(1)	Outside County Nonrequested Copies Stated on PS Form 3541 *(include sample copies, requests over 3 years old, requests induced by a premium, bulk sales and requests including association requests, names obtained from business directories, lists, and other sources)*	8,061	8,057
	(2)	In-County Nonrequested Copies Stated on PS Form 3541 *(include sample copies, requests over 3 years old, requests induced by a premium, bulk sales and requests including association requests, names obtained from business directories, lists, and other sources)*	-	-
	(3)	Nonrequested Copies Distributed Through the USPS by Other Classes of Mail *(e.g., First-Class Mail, nonrequestor copies mailed in excess of 10% limit mailed at Standard Mail® or Package Services rates)*	-	-
	(4)	Nonrequested Copies Distributed Outside the Mail *(Include pickup stands, trade shows, showrooms, and other sources)*	138	300
e. Total Nonrequested Distribution *[Sum of 15d (1), (2), (3) and (4)]*			8,199	8,357
f. Total Distribution *(Sum of 15c and e)* ▶			12,680	12,967
g. Copies not Distributed *(See Instructions to Publishers #4, (page #3))* ▶			65	53
h. Total *(Sum of 15f and g)*			12,745	13,020
i. Percent Paid and/or Requested Circulation *(15c divided by 15f times 100)* ▶			35%	36%

* If you are claiming electronic copies, go to line 16 on page 3. If you are not claiming electronic copies, skip to line 17 on page 3.

UNITED STATES POSTAL SERVICE®

Statement of Ownership, Management, and Circulation (Requester Publications Only)

16. Electronic Copy Circulation	Average No. Copies Each Issue During Previous 12 Months	No. Copies of Single Issue Published Nearest to Filing Date
a. Requested and Paid Electronic Copies ▶	5,138	5,737
b. Total Requested and Paid Print Copies (Line 15c) + Requested/Paid Electronic Copies (Line 16a) ▶	9,619	10,347
c. Total Requested Copy Distribution (Line 15f) + Requested/Paid Electronic Copies (Line 16a) ▶	17,818	18,704
d. Percent Paid and/or Requested Circulation (Both Print & Electronic Copies) (16b divided by 16c × 100) ▶	54%	55%

☒ **I certify that 50% of all my distributed copies (electronic and print) are legitimate requests or paid copies.**

17. Publication of Statement of Ownership for a Requester Publication is required and will be printed in the December 2024 issue of this publication.

18. Signature and Title of Editor, Publisher, Business Manager, or Owner
Randy Stott,
Publisher & Editor-in-Chief
Randy Stott

Date: 10/1/2024

I certify that all information furnished on this form is true and complete. I understand that anyone who furnishes false or misleading information on this form or who omits material or information requested on the form may be subject to criminal sanctions (including fines and imprisonment) and/or civil sanctions (including civil penalties).

Power Transmission Engineering®

VOL. 18, NO. 8

ZERO-MAX
Tighten to 32 Nm →
6_26-A1C

ZERO-MAX
Tighten to 32 Nm →
6_26-A1C

PTE REVOLUTIONS

An AI-Automation Hub

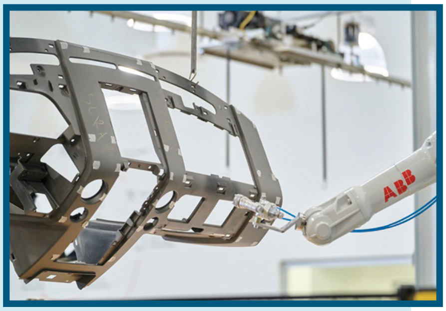

State-of-the-art doesn't begin to describe ABB's revamped robotics and training facility in Auburn Hills, MI. The upgraded factory serves as a U.S. hub for developing AI-enabled technology helping businesses respond to labor shortages, global uncertainty and sustainable manufacturing.

powertransmission.com/blogs/1-revolutions/post/10102-an-ai-automation-hub

Nord Gearmotors Helps Vincent Corporation put the Squeeze on Almost Everything

The applications are too numerous to list in their entirety. Coffee grounds. Eggshell waste. Pomegranates and pineapples. Manure and paper mill sludge. Tobacco. These are just a few of the materials that require dewatering, a process that—as its name suggests—separates fluids from solids, often converting what would otherwise go down the drain or end up in a landfill into saleable products.

powertransmission.com/blogs/1-revolutions/post/10088-nord-gearmotors-helps-vincent-corporation-put-the-squeeze-on-almost-everything

AS SEEN IN *GEAR TECHNOLOGY*

Cutting-Edge Clean

The importance of clean air in manufacturing is often underestimated, yet it's one of the critical elements that can impact both production efficiency and employee well-being. This is particularly true in facilities that rely heavily on CNC machining, where oil mist and coolant byproducts can create significant air quality challenges. Wolfram Manufacturing, based in Austin, has addressed this challenge head-on by integrating advanced mist collection systems into its operations.

geartechnology.com/articles/30810-cutting-edge-clean

powertransmission.com

AGMA MEDIA
1840 Jarvis Avenue
Elk Grove Village, IL 60007
Phone: (847) 437-6604
Fax: (847) 437-6618

EDITORIAL
Publisher & Editor-in-Chief
Randy Stott
stott@agma.org

Senior Editor
Matthew Jaster
jaster@agma.org

Senior Editor
Aaron Fagan
fagan@agma.org

GRAPHIC DESIGN
Design Manager
Jess Oglesby
oglesby@agma.org

ADVERTISING
Advertising Sales Manager & Associate Publisher
Dave Friedman
friedman@agma.org

Materials Coordinator
Dorothy Fiandaca
fiandaca@agma.org

CIRCULATION
Circulation Manager
Carol Tratar
tratar@agma.org

MANAGEMENT
President
Matthew Croson
croson@agma.org

FOUNDER
Michael Goldstein founded *Gear Technology* in 1984 and *Power Transmission Engineering* in 2007, and he served as Publisher and Editor-in-Chief from 1984 through 2019. Michael continues working with both magazines in a consulting role and can be reached via e-mail at *mwg42@hotmail.com.*

Photo courtesy of Bosch Rexroth

Natural Logo Rhythm

As publishers, we're constantly reevaluating our brand and our identity. We want our connection with you to remain close and fresh, so that when you see our publication, your reaction is, "Oh, yeah. These are my people. They speak my language."

Of course, much of that reaction is derived from the content. But some of it is also from the design and how the content is presented. Over time, designs become stale. Fonts, color schemes and visual effects that were once popular become as outdated as bell-bottom pants. (Wait, never mind. I think those are back in style again. Anyway, you get my point.)

Every once in a while, a publication needs a refresh, and that's where we're at with *PTE*. It's part of what I like to call the "Natural Logo Rhythm." In my experience a good design for a publication lasts about 10 years or so. Any longer than that and you start to risk looking like you're from the wrong decade. And for a publication focused on technology like we are, it's not a good look.

The current design for *PTE* was introduced in 2013, so it feels right to have a fresh new look.

I'm pleased to announce that *PTE* will be unveiling that fresh new look beginning in January. Right here, right now, you're getting a sneak preview of the new logo.

But it doesn't stop there. The website has been completely redesigned, with an emphasis on bigger, bolder images to highlight the technologies of mechanical power transmission as well as all of the really cool applications that rely on gears, bearings, motors, gear drives and related components. We've committed to keeping the content on our home page fresh and engaging, so that when you come to visit, you'll continue to find new and interesting articles as you scroll through the pages and explore the site.

We've also made a significant choice to distinguish between content and advertising. Moving forward, advertising and sponsored content on the website will be labeled as such. Furthermore, paid items will be placed against a subtle gray background to further distinguish them from true editorial content. In today's media world, it's hard to know what content you can trust. We believe transparency is the best way to continue earning that trust with our readers. Our editors will continue striving to bring you the most balanced, inclusive, unbiased coverage we can.

Which is not to say there's anything wrong with advertising. In fact, some of the best content we produce is provided by our advertisers, who are the most in touch with the latest technology and applications for power transmission equipment.

We're confident that you are going to love the new look as much as we do. And you can rest assured that even though we've got a fresh new set of clothes, we're more committed than ever to providing you with the highest quality technical content possible.

Please let us know what you think. And if you ever feel like we're NOT speaking your language, please let us know that, too. I'm always available at *stott@agma.org*.

PTE

P.S. There's a cheeky math nerd pun in the headline for this article. The engineers among you probably recognized it right away (if $e \approx 2.71828$ popped into your head when you read it, yeah, that's you). For the non-math nerds, e is a mathematical constant that is the base of the natural logarithm (not to be confused with the "Natural Logo Rhythm"). The constant e is sometimes known as Euler's number, named after Leonhard Euler, who is also, of course, the inventor of the involute curve.

Randy Stott
Publisher & Editor-in-Chief

IGUS
Components Reduce Maintenance for Portable Racing Simulator

Greaves 3D Engineering, a British company specializing in precision engineering, has introduced "The Ultimate Drivers Rig," a state-of-the-art racing car simulator designed for portability and professional performance. This innovative simulator can be folded and stored in a compact road case, allowing for easy transport to racetracks, trade shows, and corporate events. Central to the rig's design are 45 high-performance components from igus, including self-lubricating linear and drive technologies, cable carriers, and plain bearings, which help reduce maintenance requirements and improve overall reliability.

Upon opening the simulator's road case, users can roll out the chassis using integrated rollers. The structure then unfolds in a dynamic process reminiscent of a scene from a science fiction film. Three 32-inch monitors expand to provide an ultra-wide field of vision, and the driver's seat and pedal box adjust both horizontally and vertically. The simulator can replicate the driving positions of different vehicles, from the reclined stance of a Formula 1 driver to the more upright posture of a rally car driver. The simulation experience is further enhanced by haptic feedback mechanisms integrated into the steering wheel, pedals, and seat, offering users a realistic feel of the car and track.

Sustainable Design with igus Self-Lubricating Components

The Ultimate Drivers Rig is designed for flexibility and can be used in diverse settings such as racing teams, trade shows, or home environments. To meet the demands of portability and ease of maintenance, Greaves 3D Engineering prioritized reducing weight, minimizing installation space, and eliminating the need for regular maintenance. Given the complexity of the system's electromechanical framework, which includes hundreds of components, the engineers selected lightweight, lubrication-free solutions from igus.

Linear rails from the drylin W series are utilized to adjust the center console and driver's seat. These compact carriages, connected to the seat, glide smoothly on aluminum rails using bushings made of high-performance plastic. The bushings release solid lubricants during operation, allowing for frictionless movement without the need for additional lubrication.

"Our components maintain their mechanical integrity without requiring cleaning or lubrication," explains Michael Hornung, product manager for drylin linear and drive technology at igus. "Because no grease is used, the risk of dust or dirt mixing with lubricants is eliminated, which prevents the formation of deposits that could hinder performance."

Additionally, iglide G polymer bearings installed in the seat frame facilitate the self-lubricating process, reducing the environmental footprint of the simulator by eliminating the use of fossil fuel-based lubricants. This technology is estimated to save up to two liters of lubricant annually.

Enhanced Cable Protection with igus Cable Carriers

In addition to the linear technology, the simulator features self-lubricating, compact linear actuators from the drylin SHT series, which include a lead screw drive for the automatic adjustment of the seat and monitors. These components come preassembled with stepper motors and motor control systems, helping to save space and reduce design complexity.

The simulator's energy and data cables are housed within energy chains made from high-performance plastic, which protects them from excessive movement and prevents cable breaks. The installation includes twistable and telescoping e-chains from the triflex series, designed to move in multiple dimensions and ensure optimal protection for sensitive cables.

"The Ultimate Drivers Rig incorporates a total of 45 components from igus," adds Hornung. "Each one plays a vital role in enhancing the simulator's reliability, cost-efficiency and environmental sustainability."

Greaves 3D Engineering's collaboration with igus has resulted in a portable, high-performance racing simulator that meets the demands of professional users while promoting sustainability through the use of self-lubricating, maintenance-free components.

greaves3d.com
igus.com

NTN
Expands Low Friction Hub Bearing Series

NTN Corporation has expanded its "Low Friction Hub Bearing" series, with the development of two new products with low friction characteristics, "Low Friction Hub Bearing IV" and "Low Friction Hub Bearing V". These hub bearings were developed

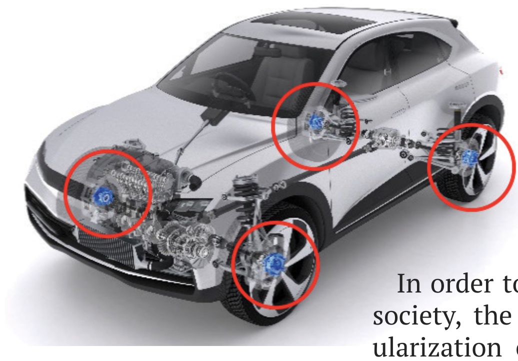

to meet the needs of the global automotive OE customer-base, as they strive to make their mobility products more efficient. These latest offerings in NTN's Low Friction Hub Bearing Series reduces rotational friction by up to 64 percent when compared to conventional designs, contributing to the increase of fuel and electrical efficiency for a wide range of vehicles including electric vehicles (EVs) and hybrid electric vehicles (HEVs).

"The newest versions of NTN's Low Friction Hub Bearings provide notable enhancements over traditional designs, helping our customers achieve their efficiency goals", said Patrick Harrell, sales director, NTN Automotive Center, "At NTN, our guiding principle is to contribute to society by developing cutting-edge technologies and products. Enhancing mobility efficiency is a perfect example of our dedication our customers and our principles."

Background of Development

In 2009, NTN developed the "Low Friction Hub Bearing", which reduces rotational friction while satisfying performance requirements such as operating life and strength. Since then, engineers have been pursuing further low friction characteristics through advancements such as reducing the number of seal lips by implementing a labyrinth structure on the inner seal and reducing grease viscosity. NTN has supplied the "Low Friction Hub Bearing" Series to OE customers and automotive aftermarket channels, and they have been highly regarded for their low friction characteristics and their contributions to improving fuel and electrical efficiency in many vehicle models.

In order to realize a decarbonized society, the development and popularization of EVs has been accelerating. To extend EV range, it is necessary for EVs to achieve further efficiencies. In response to these needs, NTN developed "Low Friction Hub Bearing IV" in 2023, an improved iteration of its predecessor, and then achieved further efficiencies with the "Low Friction Hub Bearing V," released in 2024.

Low Friction Hub Bearing IV

Low Friction Hub Bearing IV adopted a newly developed low-torque grease for the outer and inner seals. In addition to reducing the base viscosity of grease, the size of the thickener, which retains base oil and makes it semi-solid, is reduced. Reducing the size of the thickener reduces the amount of thickener required while maintaining retention of the base oil, resulting in further reduction of grease viscosity. These advancements reduce rolling resistance caused by the grease when seals are rotating and reduce rotational friction.

Low Friction Hub Bearing V

In addition to the improvements of "Low Friction Hub Bearing IV," "Low Friction Hub Bearing V" adopts the newly developed low-torque grease for the inside of bearing. While grease viscosity is reduced by reducing the base oil viscosity and thickener size, grease consistency is optimized so that the grease separated by balls when rotating will not flow back into the raceway. By implementing these advancements, "Low Friction Hub Bearing V" reduces friction by up to 64 percent compared to conventional designs. It also improves electrical efficiency in EVs by approximately 0.75 percent, enabling 1.86 miles of vehicle range compared to the conventional product.

ntnamericas.com

RULAND MANUFACTURING
Expands Jaw Coupling Line

Ruland Manufacturing has expanded its jaw coupling line to meet the demands of high-torque applications, now offering bore sizes up to 1-3/4 in or 45 mm and torque capacities of 2,655 in-lbs. (300 Nm). These new jaw couplings are designed for use in precision systems with high deceleration and acceleration curves, such as those found in semiconductor, solar, conveyor and warehouse automation applications.

With zero-backlash, industry-leading misalignment capabilities, and a balanced design that reduces vibration at speeds up to 8,000 rpm, Ruland jaw couplings deliver optimal performance for demanding environments.

Ruland jaw couplings offer the highest size-for-size torque and torsional stiffness among flexible couplings in the Ruland product line. They consist of two precision-machined aluminum hubs connected by an elastomeric element called the spider. The curved jaw profile of the hubs presses fits with the spider, ensuring zero-backlash performance. Made from advanced polyurethane material, the spider damps impulse loads, minimizing shock to the motor and other sensitive equipment.

"The expansion of our jaw coupling line allows designers to implement Ruland products in a broader

range of applications, giving them the flexibility to handle higher torque requirements with the reliability they expect from Ruland," says Bill Hewitson, president of Ruland Manufacturing. "These jaw couplings underwent rigorous physical testing to guarantee zero-backlash operation and adhere to the stated misalignment ratings, setting us apart from competitors. I am excited to support our OEM and distribution customers with these new products."

ruland.com/servo-couplings/jaw-couplings.html

MAYR
Offers Reliable Clutches and Couplings for High-Speed Applications

Based on the proven ROBA-DS steel disk pack coupling, Mayr Power Transmission developed a weight-optimized aluminum version. Compared to the steel version, the outer diameter of this new design has been reduced by up to 10 mm; the mass and mass inertia range from 40 to 60 percent of the steel version, depending on the design and size. The performance density, however, remains unchanged. It is tailored to meet the requirements of high-speed applications, for example in the field of test bench technology.

Shaft misalignment compensation couplings are decisive accessory parts in test stands, as they minimize the interference parameters affecting the measurement flange. These interference parameters or so-called parasitic forces frequently occur due to alignment errors in the driveline. This means misalignments between the input and the output sides occur in almost all applications. Shaft misalignment compensation couplings are therefore used together with the measurement flange. Here it is important that the geometric basis is correct and that the couplings are already designed for measurement flanges and high speeds in their standard version. It is important to find a balance between rigidity and elasticity in order to avoid restoring forces on the system.

The decisive criterion of Mayr couplings is that they are compact and offer high-performance density. Also designs made of steel must already be characterized by a low mass and mass inertia and at the same time achieve high speeds of up to 30,000 rpm. Then there is precision manufacturing with only a few interfaces, as well as smooth running and high balance quality. So, in general it is important that customers always consider the application when selecting the coupling and the material.

Reliable Overload Protection at High Speeds

If in a test stand the torque exceeds the limit value set on the torque limiter, the clutch disengages and separates the input and output within fractions of a second. After an overload occurrence, the measurement shaft therefore has to be recalibrated at worst, any further expensive damage to the drive line or test piece, however, is prevented reliably by the torque limiter. The EAS-HSE torque limiters by Mayr Power Transmission transmit torques backlash-free and with high torsional rigidity. Moreover, they are very compact and boast a low mass moment of inertia with a high-performance density.

The compact, high-performance design of the clutches is achieved thanks to a small outer diameter in combination with a relatively large bore diameter. And also, the integrated elements, via which the torque is transmitted on Mayr Power Transmission clutches are specially selected and symmetrically arranged. Ultimately, the following applies for the design: Bore diameter, outer diameter and element size must be harmonious in order to obtain a low-vibration system that works precisely in the event of actuation.

mayr.com

BOSCH REXROTH

Adds Force Control Feature to Mechatronic Subsystems

The Smart Function Kit Pressing, a complete mechatronic package from Bosch Rexroth for the quick realization of servo presses, is now available with force control. This means that it is now also possible to perform processes in which the target force must be kept constant over a defined period. Intelligent e-tools speed up the selection and configuration of the modular servo press. The pre-installed operating software facilitates quick and easy commissioning, process definition, and line integration.

With the newly integrated force control software feature, the Smart Function Kit Pressing covers a total of three types of applications: joining to a defined position (position controlled), joining to a defined force (position controlled), and new: joining to a defined force with subsequent maintenance of the force (force controlled).

When joining with force control, the servo press maintains a constant defined target force for a predetermined duration, even if the position of the workpiece fluctuates or its size changes. This is the case, for example, if it expands or shrinks in the process, melts, or is ground off. Continuous monitoring of the maximum force and position values protects the system and tool from damage. You can switch the curve view from force/position to force/time for better process representation and analysis.

Force-controlled joining is required in many manufacturing and assembly processes, such as in powder pressing, laser welding, or grinding. Another field of application is material testing. In battery production, for example, pouch cells are tested for tightness with constant force while the material expands with the addition of heat. In fuel cell production, the Smart Function Kit compresses components made of different materials with a defined force over a period of several minutes while introducing heat.

Save Time from Engineering to Monitoring

The correct size of the Smart Function Kit can be determined very easily using the new "-Press in/force control" reference process in the LinSelect sizing tool. Integrated safety functions (safe torque off or safe motion) are also available as selectable options in the seamlessly connected online configurator. CAD data and technical documentation can then be downloaded free of charge and the servo press can be ordered directly from the Rexroth online shop with one material number.

The Smart Function Kit for pressing and joining applications consists of the standard components electromechanical cylinder with force sensor, servomotor, drive controller and industrial PC, and is supplied pre-assembled in one package. The pre-installed browser-based operating software shortens commissioning to a few minutes, programming is done graphically via sequence modules, whereby plausibility checks prevent the system limits from being exceeded.

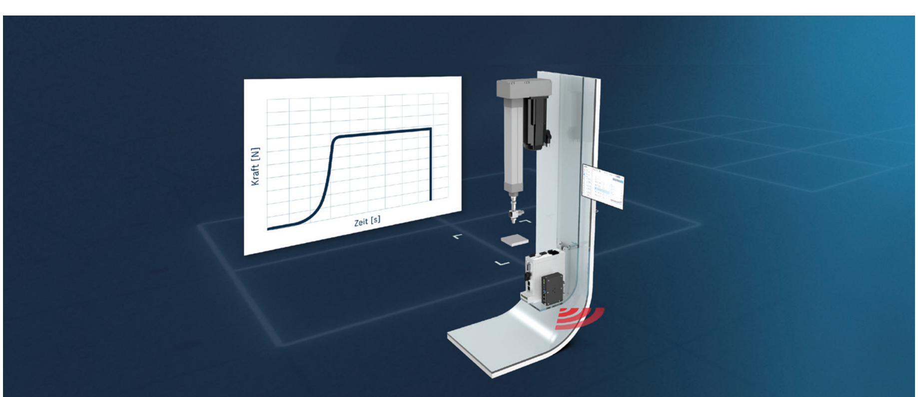

The Smart Function Kit Pressing can easily be connected to a higher-level controller in the place of use by means of prepared function blocks. From there, commands can be given to the servo press, and results and process data can be transmitted to it.

`boschrexroth.com`

SICK

Inspector83x Delivers AI Quality Control Out-of-the-Box

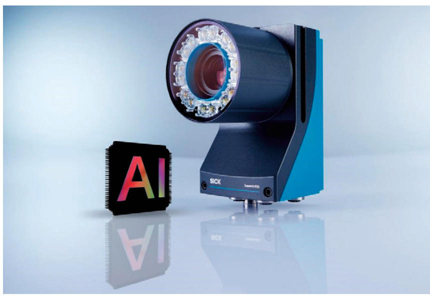

With the launch of its Inspector83x 2D vision sensor, SICK has enabled out-of-the-box AI machine vision inspections for common inline inspection tasks in demanding high-speed production.

The no-stress teach-in capability of the SICK Inspector83x can be used by non-specialists to configure powerful, high-precision AI inspections at full production speeds. By showing the camera just a handful of examples, initial inspection results can be up and running in a matter of minutes. Any product design or batch changes can be quickly added in the same way by an operator from the production line.

Simplicity and Power in High-Speed Production

With up to 5 MP resolution and powerful built-in illumination, the SICK Inspector83x is an impressive all-in-one performer. With its powerful quad-core CPU and high-speed data transfer over industrial networks, the Inspector83x processes AI inspections directly on the device, and at significantly faster speeds than its predecessors. Its highly accurate and fast response, with no need for an external machine control, is expected to be particularly useful in demanding FMCG production applications. Typically, up to 15 inspections per second can be accomplished reliably for machine vision tasks such as defect and anomaly detection or classification.

With the SICK Inspector83x, manufacturers can solve machine vision inspections with unprecedented ease and confidence, while depending on highly reliable results in applications such as consumer goods manufacture, food and beverage, automotive and packaging applications. The SICK Inspector83x masters complex inspections of medium to large scenes with ease, including evaluating products with unpredictable features and verifying complex assemblies, as well as OCR/OCV reading and verification. Additional product rollouts during 2024 include color imaging for inspection of vivid features suitable for color sorting, defect detection and quality assurance.

AI Machine Vision for Nonspecialists

Pre-installed with the *SICK Nova* foundation software, the Inspector83x offers simplicity out-of-the-box. Neither specialist machine vision expertise nor lengthy problem-solving is required to specify an inspection successfully. Using a standard PC connected via the camera‘s USB-C port or network interface, users follow the intuitive interface to present examples to the camera in actual production conditions, then train and execute the inspection. As little as five examples may be needed. Combining the AI function with conventional rule-based tools, e.g., to add a simple measurement value, allows inspections to be configured in the most pragmatic way.

The SICK Inspector 83x can eliminate conventional machine vision complexity whenever changes to product designs or packaging are needed. Rather than having to call on a machine vision specialist or external consultant to problem-solve and specify complex rule-based inspections, nonskilled operators can simply add a new product example, and the camera will learn by itself.

For complex scenes with many more examples and large datasets, users have the option to access the computational power of the SICK dStudio cloud service to train their own neural network, which can then be exported as a small file to run on the Inspector83x. With *SICK Nova*, advanced users can also expand custom developments further using Lua programming and HALCON. The SICK cloud-based dStudio service also offers the unique advantage of colleague collaboration and data management, still with user-simplicity at its core.

High-Speed Data Transfer with Versatile Industrial Networking

Once set up, the image inference is carried out directly on the SICK Inspector83x and results are output to the machine control as pass/fail results or sensor values. The Inspector83x is optimized for rapid data transfer in industrial networks with dual ports for EtherNet/IP or PROFINET integration. A dedicated high-speed Gigabit Ethernet port provides the capacity for high-resolution image data transfer as well as data logging or TCP/IP integration. A built-in export function can output customized configurations for common PLC types at the push of a button.

The SICK Inspector83x has seven inputs and five outputs. The on-board delay and queue capability precisely calibrates the camera‘s image outputs based on either time or encoder inputs to activate connected machine controls e.g. to trigger a reject pusher.

Although the SICK Inspector83x operates well as a stand-alone device, a broad range of accessories is available where required for the installation. A dedicated port for illumination can connect to external light sources such as backlights or bar lights. A near infrared (NIR) variant will be available later in 2024. Using a standard C-mount threading, customers can fit a range of optics from SICK, as well as having the freedom to fit specialized third-party lenses for complex inspections.

`sick.com`

5 Ways to Save Money Through Ultrasonic Analysis

Motion examines cost savings for aging equipment

Kristi Giba-Reiss, Motion

Figure 1—Handheld ultrasonic devices like this will show dB readings, which is especially helpful in noisy environments. Image courtesy of SDT Ultrasound.

When facilities are designed and built to meet the standards of the day, the plant is as efficient as it will ever be on day one. However, as the plant ages and production demands increase, aging equipment becomes strained leading to inefficiencies and escalating costs.

Utility expenses continue to rise with overall demand. Loads change, hold-down hardware loosens and maintenance intervals slip—causing equipment to operate below desirable parameters. Compounding these costs, threads back off on pipe fittings. Stress and strain can cause pipe fissures, and if the pipes are transporting gases, the leaks are not always easy to find.

Addressing these weak spots in your facility creates the potential for significant cost savings. While our human senses may not always be sufficient to identify these issues, various tools can help. One effective method is ultrasonic analysis, which can help identify and resolve these challenges.

Why Ultrasonic Analysis?

Ultrasonic analysis uses high-frequency sound waves, typically beyond the limit of human hearing at 20 kHz, to detect, analyze and interpret the properties of materials, structures or mechanical systems. An essential tool in multiple industries, it can detect flaws, measure thickness and ensure quality control without damaging materials. Its versatility and ease of use allow companies to follow many avenues to cost savings and enhance operational uptime.

Here are the five most effective strategies for reducing costs through ultrasonic analysis:

1. Decrease Compressed Air Costs

With a cost of over 40 cents per kilowatt-hour (kWh) in some areas, producing compressed air can greatly impact your bottom line. Add the fact that a rotary screw compressor can generate 3–4 cubic feet per minute (cfm) per kW, and air costs become quickly apparent.

Compressed air, often dubbed the "fourth utility," is the most widely utilized resource in industry due to its versatility. As a plant ages, many factors can cause inefficiencies in this system, accounting for up to 50 percent of the compressor output. Maintenance teams often overlook air leaks as they don't typically make a mess on the floor, don't always affect production and are invisible. Noises from the production floor can mask the sounds of compressed air hissing out of cracks, loose fittings and failed valves. This is where ultrasonic analysis comes in. (Figure 1).

An ultrasonic analysis device fitted with headphones and a directional attachment can help isolate the sounds of the leaks (typically around 40 kHz). Depending on the attachment, you can scan up to 300 feet away. Listen for higher-pitched sounds as you sweep the attachment toward the pipes—the leaks are evident where the decibels (dBs) peak as identified with your headphones.

For Related Articles Search
ultrasonic
at powertransmission.com

Figure 2—As steam travels turbulently through the pipes, an ultrasound device can "hear" the movement of the steam, providing valuable insights into its flow and behavior. Image courtesy of Motion.

As leaks are repaired, the load on the compressor decreases, lowering operating costs and sometimes allowing the end user to benefit from utility provider incentives. Ideally, a team would regularly handle compressed air monitoring and leaks (often biannually). If your plant has not conducted a compressed air survey in the past 3–5 years, consider this opportunity to save upwards of tens of thousands of dollars.

2. Prevent Costly Mechanical Failures

Unplanned downtime is expensive. Prevent expensive disruptions by implementing condition monitoring and conducting regular inspections to maintain awareness of your assets' condition—especially the most critical ones. Ultrasound technology can detect friction, turbulence and impacts earlier than any other monitoring method, allowing your maintenance team to take proactive maintenance measures before issues escalate into major concerns.

Begin monitoring bearings by establishing a baseline. An accurate baseline for healthy equipment is crucial as there is no "typical" decibel range for bearings. If the asset is already in a state of decline, a baseline can be taken from the same type of bearing operating under similar loads. Once a baseline is set, take readings with your ultrasound device by placing a sensor at the top of the bearing housing (the same place where you established your reading). If you observe a dB gain of 8 or more, it's time to investigate. Once the gain doubles, it indicates bearing degradation, making it imperative to order repair parts. A 30 dB gain increase over the baseline is a forewarning of potential catastrophic failure.

To identify the cause of a dB gain, perform additional analysis in the recording's FFT timewave form on an advanced device. For instance, repetitive dB spikes often indicate bearing imperfections, while inconsistent spikes could indicate under- or over-lubrication.

3. Optimize Greasing Activities

If your facility lacks a well-maintained and proactive maintenance program, your bearings likely do not receive the right amount of grease. Establish a lubrication route to identify the amount of grease required based on current loading and update the requirements if any conditions change. Traditionally, plants have not taken baseline readings of assets when new (as described in the previous section).

Facilities can mitigate these pitfalls by adding an ultrasonic greasing attachment to a grease gun. The same handheld unit used for identifying air leaks can also be modified for greasing purposes. To use an ultrasonic grease gun, start by placing a contact sensor on the bearing housing to establish a baseline. As you pump grease, the dB level will begin to lower. Continue to gradually apply grease until the dB level slightly increases. If your device has a route programmed into it, you can set this as your optimal amount of grease, and it will remind you when your next maintenance cycle is required. Achieving the optimal grease level results in smoother operations, extending the life of the bearing and the parent asset.

4. Reduce Steam Usage

Steam systems are commonly used in manufacturing, food refining and meat processing. Like compressed air, steam is expensive to produce, and leaks are difficult to detect. Steam is crucial to cleaning and various processes, such as pasteurization, where the quality of steam is vital. Pure steam cools as it progresses from boilers to the intended point of use, forming a mix of condensate and gases. To maintain steam purity, steam traps are installed to capture and remove the condensate and waste that accumulate in the system. These traps are intended to modulate automatically, discharging condensate as it is formed to ensure consistent purity and efficiency throughout the system. However, steam traps with moving parts are failure-prone, potentially leading to up to 30 percent of waste in the system.

Ultrasound technology, capable of measuring turbulent flow even through thick pipe walls, can effectively monitor the progression of steam throughout the system.

As steam travels turbulently through the pipes, an ultrasound device can—under normal conditions—"hear" the movement of the steam, providing valuable insights into its flow and behavior (Figure 2).

When a steam trap fails, the valve can be stuck in the closed or open position, or it might flutter between the two. Each condition produces different ultrasonic signatures around the 25 kHz range. By simply pointing the directional device toward the steam trap and surrounding lines, you can listen for signs of turbulent flow. If the flow is nonexistent or cycling rapidly, it indicates that the team must replace or repair the trap.

5. Detect Hydraulic Leaks

Hydraulic systems convert electric power to mechanical energy using hydraulic fluid. These systems consist of pumps moving hydraulic fluid from a reservoir through high-pressure lines. Control valves direct the fluid, cylinders produce mechanical energy, and relief valves are included for safety. Hydraulics systems are often used in areas needing high pressures, but leaks, blockages and bypasses can restrict the system from producing the required power. These hydraulic unit issues could lead to malformed products, slower movement, increased lubricant consumption, downtime and potential environmental penalties.

Ultrasound technology can detect failure modes in hydraulics systems, such as bearing defects, cavitation and fluid leakage past valves or the head or wiper seals. If possible, establish a baseline by taking measurements of a "new" system; this will allow you to compare current conditions with best-case scenarios. Whether or not you have a baseline, you can use an ultrasound probe to listen to the airborne noise level (in A-weighted decibels, or dBA) about 1 meter (3 feet) downstream from the potential failure points. The most common components to test for leaks are valves, cylinders and pumps, and failure will result in the symptom of a higher-pitched sound compared to the surrounding areas. For bearing related concerns, refer to points 2 and 3 above.

Ultrasonic analysis is not only a method for ensuring safety and quality but also a powerful tool for cost savings. From preventing costly equipment failures to reducing material waste and avoiding regulatory fines, the financial benefits of ultrasonic analysis can significantly impact a company's bottom line. Integrating this technology into maintenance and production processes enables businesses to achieve greater efficiency, reliability and cost-effectiveness.

The information in this article serves as a solid starting point. To ensure the best results, engage a qualified professional trained in predictive maintenance. Your bottom line and your company will thank you.

Motionind.bizMiPTE245

PTE

Revolutionizing Conveyor Belt Technology in Food Processing

Regal Rexnord upgrades operational efficiency with MP Equipment

Regal Rexnord

Mike Mitchell at Middleby Food Processing helped develop a patented Beaver Tail End design, which allows for smoother product transition, enhancing operational efficiency. All photos courtesy of Regal Rexnord.

With over 20 years' experience in the food processing industry, Mike Mitchell has filled many roles in his career. Now, as the key accounts manager for Middleby Food Processing brand, MP Equipment, Mitchell has been pivotal in advancing food technology. He understands the demands of frequent, late-night repairs on first generation equipment.

"I've been that production guy at three o'clock in the morning underneath the breader or the fryer, dealing with the problems no one wants to deal with," said Mitchell, who began his food processing career in a poultry factory.

Not only does he have insight due to his past experience, he's now in an interesting position to innovate the next generation of technology that saves end users oil costs while making repairs simpler and safer for workers. Mitchell and the engineering experts at MP Equipment have recently developed an exciting new batter, breader, and fryer line that integrates technology from Regal Rexnord and fellow Middleby brand, Filtration Automation.

Most notably, the team developed a patented Beaver Tail End design which added the belt path to the next conveyor, replacing outdated sliding mechanisms. This feature allows for smoother product transition, enhancing operational efficiency. Additionally, the introduction of a unique sediment belt in the U.S. market plays a crucial role in maintaining oil quality by removing floating debris like chrome, which reduces oil degradation and maintenance frequency, thereby increasing uptime.

The fryer's integration with advanced Filtration Automation further aids in oil management by ensuring active movement and cleaning of oil, especially in typically stagnant areas, through targeted jet flows. This not only saves on oil costs but also extends the oil's life and quality.

"We developed the Beaver Tail, and were looking for a vendor to help us make that concept become a reality," Mitchell said. "We had tried many different belts, and we were looking for what lasts the longest, what is the easiest for the customer to repair, what is the fastest to repair."

With its robust design, the Regal Rexnord PacTitanPro belt significantly extends component lifespan while reducing the frequency of replacements. Engineered to splice together easily with a pin, it minimizes the need for direct handling, enhancing worker safety.

Traditional belts, prone to frequent breakdowns and labor-intensive maintenance, posed significant

In specific processing scenarios such as battering and frying, Regal Rexnord PacTitanPro belt optimizes the use of resources like batter and oil, which reduces waste and decreases the cost of materials.

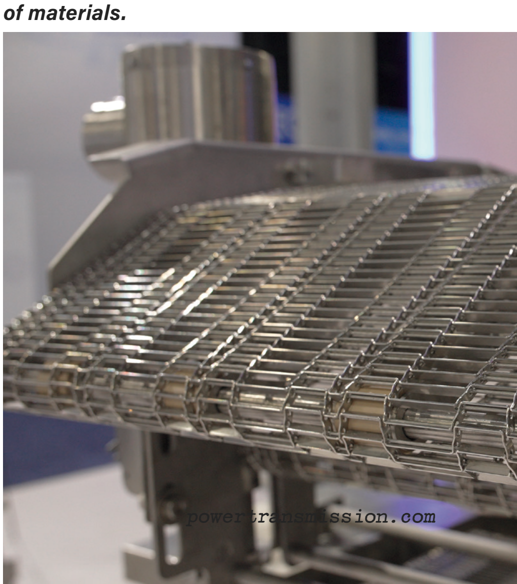

challenges. The need for regular splicing not only increased downtime but also introduced safety risks, with exposed wires leading to potential cuts and lacerations.

"When we found this PacTitanPro belt, we found that it has a simple pin that slides through, you can hold it with pliers while you slide the pin through, you don't even have to touch the belt with your hands," Mitchell said. "So, it's able to perform under these hot, oily conditions a lot better than any of the other belts we tried."

The PacTitanPro design also ensures that any broken pieces are contained, preventing contamination of food products. This innovation not only improved safety and reduced maintenance time but also contributed to lowering the total cost of ownership for end users by decreasing downtime and increasing production efficiency.

The sustainability and cost efficiency of the PacTitanPro are also noteworthy. Its stainless-steel construction and innovative design extend its service life up to six times longer than traditional metal belts, dramatically reducing the frequency of replacements and minimizing environmental impact.

In specific processing scenarios such as battering and frying, the belt optimizes the use of resources like batter and oil, which not only reduces waste but also decreases the cost of materials. The flat wire design of the belt creates a ploughing effect in frying applications, ensuring efficient

Natalie Gray assisted with sourcing additional components like motors, speed reducers and bearings into MP Equipment's applications.

oil usage and maintaining the quality of the food processed.

"By integrating oil cost reducing technology from Filtration Automation with our MP fryers, we've revolutionized oil management. We've made sure it's continuously cleaned and circulated, eliminating stagnant spots and extending oil life," Mitchell said. "So not only does this reduce oil costs, but it also guarantees that the food quality remains consistently high, preventing nutrient loss and maintaining flavor integrity."

MP Equipment tested the new Beaver Tail innovation at an Arkansas poultry processing facility. There, the new integrated system was subjected to rigorous conditions for six months and showed no failures, even under high tension and harsh environments. It lasted 12 times longer than the previous belt solution used at the facility, dramatically reducing maintenance time and costs associated with belt replacement.

Following the successful integration of the PacTitanPro, Mitchell worked with Regal Rexnord's Natalie Gray to source additional stainless steel, IP69-certified components for MP Equipment applications, including a Leeson electric motor, Boston Gear speeder reducer and SealMaster bearings.

Regal Rexnord drives efficiency and throughput for conveyor applications across countless industries, from food processing and beverage bottling to mining and material handling. Collaborative, solutions-based engineering is what sets Regal Rexnord apart, Gray said.

"We know the components, but we also know how they work together in the entire system. We really are system experts," she said. "We work with our partners to come up with comprehensive, well-engineered solutions to whatever pain point they're trying to solve."

In the end, the collaboration between MP Equipment and Regal Rexnord not only solved a pressing engineering challenge but also set a new standard in the industry.

"We've had the best time working with Regal Rexnord all the way through this, our salespeople to the engineers that have worked with us not on just this product line," Mitchell said. "They are in our hip pocket all the way through this, we really can count on them as a partner."

regalrexnord.com
mpequipment.com
PTE

For Related Articles Search
food and beverage
at powertransmission.com

Operational Improvements

A Conversation with Solve Industrial Motion Group CEO, Ernie Lauber

Matthew Jaster, Senior Editor

Since taking over as CEO of Solve Industrial Motion Group in June 2024, Ernie Lauber has focused on continuous improvement, predictive maintenance and growing the legacy brands within Solve.

Combining brands such as IPTCI, MasterDrive, PTI and TRITAN together with the LMS, SST, SPB-USA and USA Roller product lines, Solve Industrial Motion Group is a provider of high-quality metric and American Standard power transmission components and industrial-grade bearings.

With a comprehensive product catalog, highly honed supply chain, ISO 9001 certified quality control, advantageous pricing and the ability to custom manufacture bearings and components to fit virtually any need, Solve delivers products to meet demanding service requirements in areas such as agriculture, automotive, mining, aggregates, material handling, food and beverage, forestry/wood products and more.

Ernie Lauber, CEO, Solve Industrial Motion Group.

A Focus on Continuous Improvement

Lauber's career has prepared him for this role as CEO in the mechanical power transmission market.

"I'm a mechanical engineer undergrad, a tactile, hands-on, visual person, right? My mechanical background has always served me well, problem solving, critical thinking, analytical, etc.," Lauber said. "I spent 20 years at Danaher, and, you know, I saw the company grow from 1 billion to 24 billion. This really afforded me the ability and experience to fill my toolkit."

Lauber said he has a knack for unlocking potential. "Aspirational growth, continuous improvement, everything I do is rooted in the customer. Where is the transformation? Where does it happen? I've sat in a variety of seats from product management to manufacturing to strategic marketing to senior sales leader. I took on a president's role for a company called JBT Food Tech, a big vertical in the food processing industry. Capital equipment manufacturing and heavy aftermarket really prepared me for this opportunity at Solve."

Specific to the CEO role at Solve Industrial, Lauber is setting his own personal and company goals for continuous improvement and brand growth.

"What's going on here is rather unique. There have been five acquisitions in the last three years—really strong brands—and in the next two to three years, we want to double this. It's about being a platform, a destination, and a one stop shop for bearing and power transmissions solutions," Lauber added. "There's been heavy investment in a 300,000 square foot distribution center in Charlotte. We've invested in a new director of engineering and an engineering team, as well as the addition of myself and some other senior leaders."

Market Challenges and New Technologies

In terms of specific challenges in mechanical power transmission, Lauber cites the global supply chain and talent acquisition as two areas in need of attention.

"This supply chain has a heavy global component and a heavy Asian component. We've made investments in people, trading partners and in Asian manufacturing, so we feel that we've got good feet on the street and the right investments," Lauber said.

"We're going to be further diversifying, outside of China, outside of Taiwan, and making sure we've got a well-balanced, manufacturing portfolio. We're also being aggressive with manufacturing here in the United States and we're going to be expanding that."

By hiring new leadership and engineers, Solve Industrial will transform into an integrated, flexible destination for talent.

"It's one thing to be a $20 million, multigenerational, family-owned company, but now, when you bring in five, six, 10, acquisitions and integrate them into our portfolio strategy it's about growth for the entire organization," Lauber said.

Solve Industrial Products

The following is a summary of a few of the product categories Solve Industrial Motion Group provides in mechanical power transmission:

Ball Bearings

Radial/Deep Groove Ball Bearings are the most common and versatile bearings. Engineers choose them for their efficiency, durability, and low maintenance needs. Their deep raceways enable them to support both radial and axial loads, making them versatile for applications requiring high speed and precision. Solve's radial/deep groove bearings are made from high-quality AISI-52100 chromium bearing steel as well, many are also produced with 440C Stainless Steel, which is ideal for corrosive and food grade applications.

Spherical Roller Bearings

Spherical Roller bearings utilize two rows of rollers operating in a common sphered outer ring raceway. This design provides a self-aligning solution that is the combination of a radial & thrust bearing that operates even if the shaft and housing are, or become, misaligned under load. This high-capacity bearing performs consistently in adverse conditions such as shock loads, shaft deflections, marginal lubrication, extreme speeds, contamination, and critical application stresses. To enhance lubrication efficiency, the outer ring of these bearings features an annular groove and lubrication holes (W33). C3 internal clearance provides component expansion during operation at moderate temperatures.

MD Flex Couplings

Solve's MasterDrive brand flexible couplings are ideal for accommodating shaft misalignment, reducing vibrations, and transmitting torque smoothly. They enhance machinery performance, prevent damage, and extend the lifespan of connected components. Features include: No lubrication or maintenance needed; quick and easy installation; allows for 4-way flexing: angular, parallel, axial, and torsional; smooth operation and quiet performance. MD Flex couplings are available in coupling sizes 3-14. Inserts are available in multiple materials, including EPDM, Neoprene, and Hytrel.

Jaw Couplings

Jaw Couplings are an excellent choice for applications that require a low-cost, general-purpose coupling. They allow for a quick and easy shaft-to-shaft connection method. Solve's portfolio of jaw type couplings provide efficient power transmission of torque, compensate for misalignment, and protect equipment from shock loads, enhancing overall machinery reliability. Two coupling hubs are used in pairs with an elastomer element (spider), each sold separately. The element eliminates metal-to-metal contact and acts as a shock absorber. The design is considered "fail-safe" because if the element fails, the load would still be carried by the hubs. Jaw couplings are available in sizes L035-L225. Available element materials include Buna-N (Rubber), Urethane, Hytrel, and Bronze.

Mounted Ball Bearings

Solve offers the widest assortment of mounted bearings and ball bearing inserts in the industry. They stock popular Metric and American Standard configurations with bore sizes up to 140mm or 4". Solve is unique because it's one of the few companies that make four different types of locking collars for bearings. These types are set screw, eccentric locking collar, concentric locking collar, and adapter lock.

V-Belt Sheaves

Solve precision engineers a comprehensive range of single and multi-groove V-Belt Sheaves in a variety of configurations from bored-to-size and H bushed to the durable heavy-duty QD sheaves. These sheaves and bushings exceed the stringent ASTM/SAE specifications for gray iron casting. The team accurately machines each piece from high-quality gray cast iron and ensures static balance. To ensure performance, they also perform a phosphating process before painting to boost rust resistance and paint adhesion. This process yields a durable, baked enamel finish that allows for smooth, trouble-free functionality.

Timing Pulleys

Some systems can't afford to have any slippage. Solve's Timing Pulleys and Belts work together perfectly, much like gears. Timing Pulleys have teeth that lock in with a corresponding toothed belt. This setup allows your machines to run at higher speeds, work more efficiently, and doesn't require lubrication. Plus, they are more convenient for places where it's hard to do maintenance. Solve offers Timing Pulleys and HTD Pulleys in various sizes and styles. This includes 'L' and 'H' Pitch as well as HTD (5M, 8M & 14M) configurations. They are supplied in solid, webbed, or spoked designs depending on size and series.

Condition monitoring and predictive/preventative maintenance will be areas that should offer technology benefits moving forward.

"Has IIoT evolved like everyone thought it was going to because of firewalls and data and all the cybersecurity risks? Maybe not, but what it has done is helped us in the MRO space. So now people have a better understanding from a predictive standpoint when you need to replace components based on vibration, heat and all these other factors," Lauber said.

Lauber also sees great potential in AI.

"As far as understanding the needs of our customers today—a lot of these new software tools have an AI interface where we can recognize what kind of equipment our customers have and this lets us have a better grasp on how we properly maintain this equipment. Do they need a bearing repaired or fully replaced? AI will be extremely beneficial in the aftermarket space moving forward."

Lauber cites a very thoughtful, lean implementation taking place across Solve Industrial.

"We're starting with our Charlotte distribution center to make sure our teams are working with a kind of kaizen mentality. How do we develop the right kind of Gemba boards, the right kind of visual management. We had someone tell us we didn't need to pull any additional data other than the data that was already in front of us. I'm a data junkie, so I'm fascinated by the notion that continuous improvement is not just on the plant floor, it's also going to be in our leadership, in the review of our initiatives and how we plan to support our customers in the future," Lauber said.

Brand vs. Product

Solve Industrial has additional expansion plans in the coming years and is also working on methods to bring other PT components under the umbrella.

"We've shifted to a product category focus versus a brand focus. And that doesn't mean we don't honor and understand the legacy of our brands. We just need to examine the notion that we have different price points and value propositions in the bearing space," Lauber said.

In addition, Lauber plans to pay close attention to what the power transmission space will look like in the coming years.

"Gearboxes, material handling, new equipment builders, for example. There's plenty of opportunities for components and systems that transmit power. So, what I can tell you is, we're not just going to focus on the bearings and the sprockets. We're going to be exploring linear motion. We'll be exploring gearboxes. We're going to examine these markets to understand what is needed out there for us to be that engineering, consultative, one stop shop we discussed earlier."

While major change isn't always seamless, Lauber believes the company is making the right kind of investments for future growth.

"People are extremely excited about our long-term plans at Solve Industrial. These legacy brands will continue to provide the right solutions for the right markets. We're investing in new technologies as well as new talent. Our vision of becoming a power transmission platform is for real. The energy and passion around here have been incredible," Lauber said.

Lastly, we asked Lauber how the organization plans to evolve in the future.

"It builds upon that reoccurring theme, creating a platform, a destination, you know, and it's easy to say, it's hard to do. Suddenly you have several new acquisitions and you're growing organically. How do you maintain the kind of support and service your customers are accustomed to at a greater scale? This is how I'm challenging the team to think," Lauber added.

solveindustrial.com

PTE

The Future of Power Manufacturing, Warehousing and Logistics

A revolution driven by robotics, automation and AI

Dijam Panigrahi, Gridraster

In recent years, the power engineering manufacturing industry has been undergoing a significant modernization movement, driven by the rapid advancement of robotics, automation, and artificial intelligence. Amazon's recent announcement of its in Shreveport, Louisiana, serves as a prime example of this revolution in action.

Creating a Symbiotic Relationship Between Robots and Humans

This state-of-the-art facility, spanning an impressive three million square feet across five floors, represents a significant leap forward in the integration of robotics and AI into warehouse operations. It is also set to employ ten times as many robots as a standard fulfillment center, showcasing the company's commitment to leveraging technology to enhance efficiency and productivity.

This move is not just about replacing human workers with machines; rather, it's about creating a symbiotic relationship between humans and robots, where each complements the other's strengths. The facility will still employ 2,500 people, highlighting the continued importance of human expertise and oversight in these advanced systems.

Amplifying the Use of Digital Twins

One of the key technologies driving this movement is the use of digital twins. Digital twins are virtual replicas of physical systems, products, or processes that can be used for design, production, and training purposes. In the context of manufacturing and warehousing, digital twins allow companies to simulate and optimize their operations in a virtual environment before implementing changes in the real world. This approach significantly reduces the risk of costly errors and allows for continuous improvement of processes.

For instance, companies can use digital twins to design and test new warehouse layouts, optimizing the flow of goods and the placement of robotic systems. They can also simulate various scenarios, such as sudden spikes in demand or supply chain disruptions, to develop robust contingency plans. In terms of training, digital twins provide a safe and cost-effective way to familiarize workers with new robotic systems and processes without disrupting actual operations.

Augmented Reality (AR) and Virtual Reality (VR) technologies are also playing an increasingly important role in this new paradigm. AR can be used to provide real-time information to warehouse workers, helping them locate items more quickly and efficiently.

VR, on the other hand, can be used for immersive training experiences, allowing workers to practice complex tasks in a safe, virtual environment before performing them in the real world.

Embracing 3D-AI Solutions

The concept of 3D-AI is emerging as a crucial element in tying all these technologies together. 3D-AI refers to the use of artificial intelligence algorithms to process and analyze three-dimensional data, such as that generated by digital twins and AR/VR systems. This technology enables more sophisticated decision-making and predictive capabilities, further enhancing the efficiency and responsiveness of manufacturing and logistics operations.

For example, 3D-AI can be used to optimize the movement of autonomous mobile robots (AMRs) within a warehouse, ensuring they take the most efficient routes and avoid collisions. It can also be employed to analyze the 3D structure of products and packaging, automating the process of determining the best way to stack and transport items. Furthermore, 3D-AI can be used to analyze data from multiple warehouses and distribution centers, optimizing the entire supply chain network in real-time.

Amazon's use of the Sequoia system in its new fulfillment center is a prime example of how these technologies are being implemented today. Sequoia is a multilevel containerized inventory system that can hold over 30 million items, making it faster and safer for employees to store and pick goods. This system, which is five times larger than the one deployed in Houston last year, demonstrates the rapid pace of innovation in this field.

Another leading manufacturer embracing these technologies is Siemens. The company has developed a comprehensive digital twin platform that covers the entire product lifecycle, from design and production to maintenance and optimization. Siemens uses this technology not only in its own manufacturing processes but also offers it as a solution to other companies looking to digitize their operations.

Overcoming Workforce Development Challenges

While these technological advancements are crucial for the future of manufacturing and logistics, it's important to recognize that they also present challenges, particularly in terms of workforce development. As the demand for skilled workers who can operate and maintain these advanced systems grows, companies are facing a significant skills gap.

To address this challenge, U.S.-based companies should consider partnering with friendly nations like India for workforce development opportunities. India, with its large pool of skilled IT professionals and engineers, can provide valuable resources to help bridge this gap. By leveraging India's technological expertise and workforce, U.S. companies can continue to expand their operations despite current labor challenges.

For instance, companies could establish training centers in India to develop a workforce skilled in operating and maintaining advanced robotic systems and AI algorithms. These workers could then be deployed globally or work remotely to support operations in the U.S. and other countries. Additionally, Indian tech companies could be engaged to develop software and AI solutions for manufacturing and logistics applications, fostering a mutually beneficial partnership.

However, it's important to strike a balance between leveraging global talent and developing domestic capabilities. Companies should also invest in STEM education and vocational training programs within the U.S. to ensure a sustainable pipeline of skilled workers for the long term.

Moving Ahead into the Future of Manufacturing

As we move into the future, the integration of robotics, automation and AI into manufacturing, warehousing, and logistics will become increasingly sophisticated. We can expect to see more facilities like Amazon's Shreveport fulfillment center, where robots and humans work seamlessly together, guided by advanced AI systems and digital twins.

For Related Articles Search
IIoT
at powertransmission.com

The use of AR and VR for training and operations will become commonplace, enhancing worker productivity and safety.

Moreover, the concept of "lights-out" manufacturing, where entire production lines operate without human intervention, may become a reality for certain industries. However, human expertise will remain critical for oversight, maintenance, and handling complex or unique situations that AI and robots may struggle with. New research from Interact Analysis shows that the global warehouse automation market will grow from $29.6 billion in 2020 to $69 billion in 2025.

The supply chain of the future will be more responsive and resilient, thanks to the predictive capabilities of AI and the flexibility offered by advanced robotics. Real-time data analysis will allow companies to anticipate and respond to changes in demand or disruptions in the supply chain almost instantaneously. This increased agility will be critical in an increasingly volatile global market. As we move forward, the companies that can effectively integrate these elements will be the ones that lead the way in shaping the future of industry.

gridraster.com

PTE

When off the shelf just won't do.

With our extensive range of standard components and custom machining capabilities, a custom-designed and manufactured gearbox for specific applications is something we do all the time.

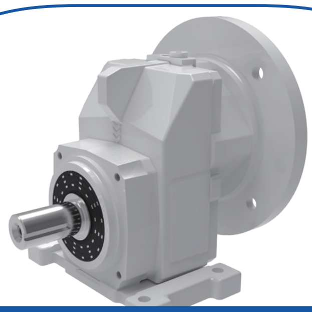

FDA Paint

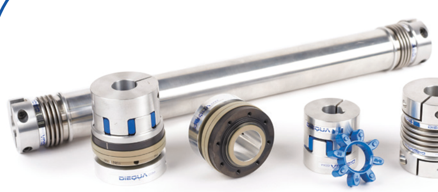

Stainless Couplings

Stainless Spindles

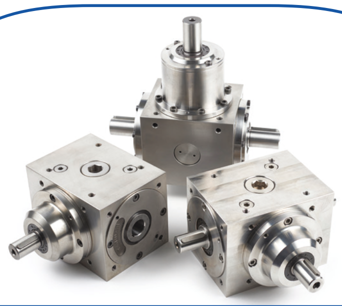

Stainless Housings

DIEQUA Corporation

180 Covington Drive
Bloomingdale, IL 60108 USA
630-980-1133
www.diequa.com

Motion Control and Power Transmission Drive Components

Engineering sMart

Your resource for the latest in great ideas from our advertisers. Check this section every issue for sMart Engineering ideas and technology.

For information about advertising contact

Dave Friedman
(847) 437-6604 | *friedman@agma.org*

Subscribe TODAY

IT's FAST. IT's EASY.
IT keeps YOU in the KNOW.
powertransmission.com/subscribe

Control System Techniques—Dampers (Part 2)

Donald Labriola II, PE—QuickSilver Controls Inc.

Closed-loop control systems can handle a wide range of motions with a wide range of loads if the control system and the mechanics of the system are properly designed for the task. A couple of the more difficult combinations to design for are high inertial mismatches and backlash with hard gearing. The question is not just how to make the system stable but also how to get the desired performance.

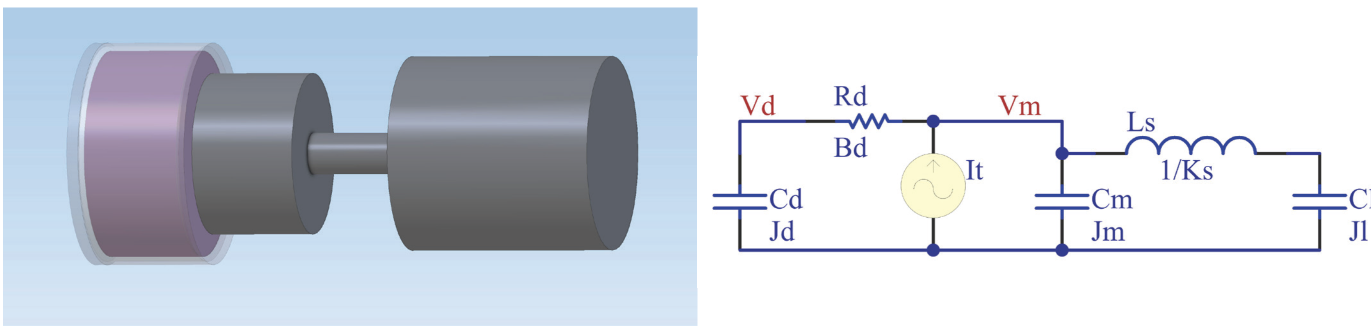

Figure 1—Damper attached to motor inertia, shaft, and load inertia (left). Electrical model of damper with motor inertia, torsion spring and load inertia (right).

Physical Viscous Inertial Damper

In "Control System Techniques—Dampers (Part 1)" [*PTE*, Vol. 18, No. 7; October 2024] we showed how adding a mechanical damper to a motor/load mass section reduces the resonance peaking in the system. In addition to reducing the peaking, a damper raises the system's phase margin. The combination of reduced resonance peaking with more phase margin allows the gain of the system to be increased significantly. We will get back to this, but more gain allows for wider bandwidth and tighter control of the load. More gain/bandwidth is also one of the fundamental ways to deal with stiction.

We will continue with the motor/damper/high inertia system. A physical viscous inertial damper (Figure 1) is shown mounted to the motor inertia (stiff compared to the viscous coupling of the grease), with the 100:1 inertia attached to the motor via a shaft. The impedance of the damper is to the left of the current (torque source), while the motor inertia, shaft torsion, and load inertia are shown to the right of the torque source in both the schematic and physical representations.

Whenever the motor velocity is greater than the damper inertia velocity, shear occurs in the viscous oil coupling them inside the damper, and the net torque available to accelerate the motor and load is reduced. Similarly, whenever the damper inertia velocity exceeds the motor velocity, the damper supplies torque into the system. Rapid changes in velocity, such as due to resonance, cause more shear and greater dissipation of vibrational energy into the viscous grease, removing the vibrational excitations from the system.

The improved gain and phase margins of the system allow for higher gains, reduced error and higher speed operation (wider bandwidth). The undesired part is that the damper is typically on the order of half or more of the size of the motor, and often a couple of times more expensive!

Synthetic Inertial Damper

This improvement in system performance without the added cost was the basis of wanting to simulate the viscous inertial damper in software. In electronics, there is a concept of Norton to Thevenin Equivalent circuits. In this transformation, a current source (or torque in the mechanical system) and the impedance representing the motor and load inertias, and shaft spring constant, can be converted to a voltage (mechanical velocity) with the impedance in series. When an additional load is then added, the current through the load (torque coupled to the mechanical damper) can be calculated as the voltage (velocity) divided by the sum of the motor/shaft/load series impedance and the added damper impedance (Thevenin equivalent circuit). In software, we can (real-time) simulate the torque that would be needed to accelerate the damper inertia to the motor velocity, given the measured motor velocity. The torque so estimated can then be subtracted from the commanded torque to the motor (from the rest of the control loop) so that the motion of the motor with the synthetic (simulated) viscous inertial damper closely approximates that of the motor and load with the physical inertial damper attached. This simulated damper gives the same improvements in gain and phase margins of the system as would the physical inertial damper but without the size and cost disadvantages.

Of course, nothing is quite free. The stepwise output of a rotary encoder and the time lag involved in processing reduce some of the margins and require a bit more complexity, but in many cases, the approximation is very good and the improvements are substantial.

In the previous article, we showed that a 100:1 inertial mismatch resulted in significant peaking at resonance (motor inertia *Jm*= 1e-5 kg-m^2, *Ks*= 100 Nm/radian ≥ *Ls*=1/K = 10-2 radian/Nm, load inertia *J1*= 1e-3 kg-m^2):

The damper inertia was selected as three times the motor inertia *Jd*=3e-5 kg-m^2, and the damping constant of the viscous oil was adjusted in the simulation to give a nice overall damping with *Bd* = 20N/Rad/sec.

The resulting system of the motor and load and damper improved the phase margin just above the resonance from -90 (for the velocity, and -180 for position) by about 120 degrees! It also reduced the peaking from 64 dB to 30.4 dB (gain of 1631 to a gain of 33.2) at resonance. We still have a phase margin of 40 degrees at 1000Hz, so the bandwidth of the system can be significantly improved.

In the system modeling, we take the voltage (motor speed) of the motor with 100 times the load inertia, and we divide it by the impedance of the (motor + inertia) plus the damper. The current (torque) transmitted by the viscous coupling in the damper is the same in this topology (which is an electrical model, as inertia is always modeled as a capacitor connected to a ground node) as in the parallel version with the current (torque source). This model is not physically realizable in the mechanical design but gives an easy method to calculate the torque absorbed by the mechanical damper attached to the motor. Note: The voltage source labeled as *Vm* in the series circuit model is the Thevenin equivalent voltage representing the speed of the motor/shaft/load without the damper present.

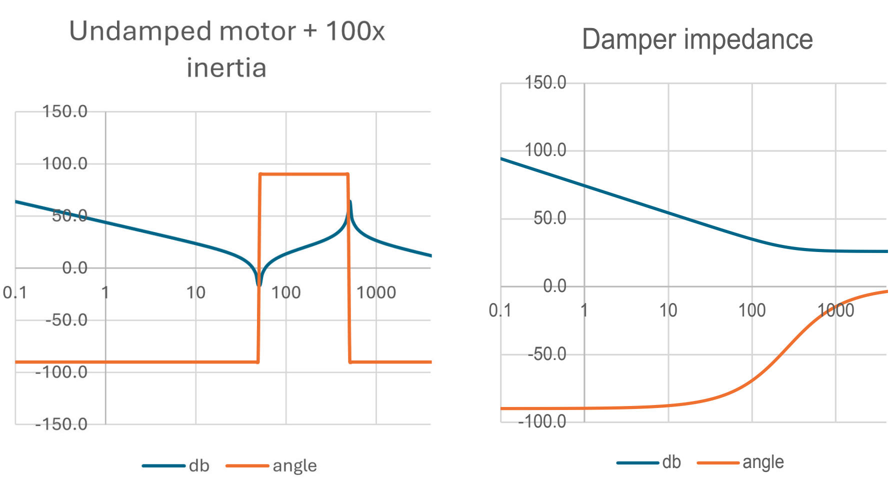

Figure 2—Impedance (velocity response to applied torque) of motor, shaft torsional spring, and 100x load inertia (left). Impedance of viscous inertial damper (right).

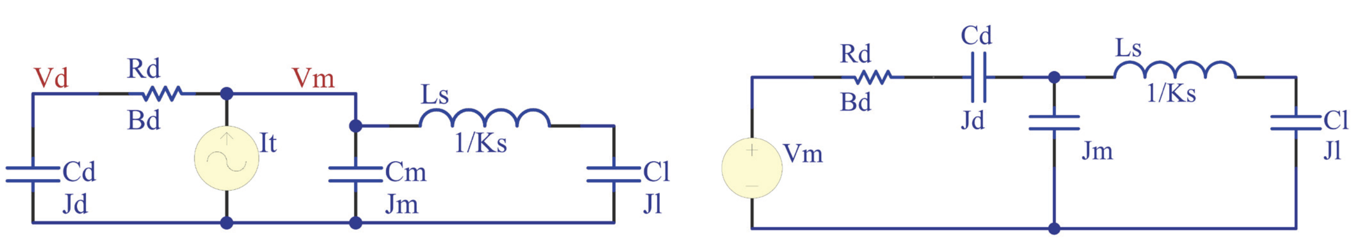

Figure 3—Electrical model of damper attached to motor inertia with motor shaft torsion spring and load inertia (left). Electrical model with Thevenin equivalent damper portion to show how spread sheet calculations were derived (right).

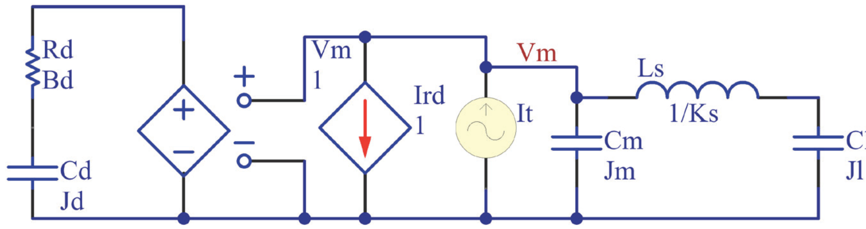

Figure 4—Electrical model with model of damper interconnected to the model of the motor, shaft and damper to implement a synthetic inertial damper. Calculated damper torque based on measured motor speed is injected into motor drive torque to produce same transfer function as an attached physical damper.

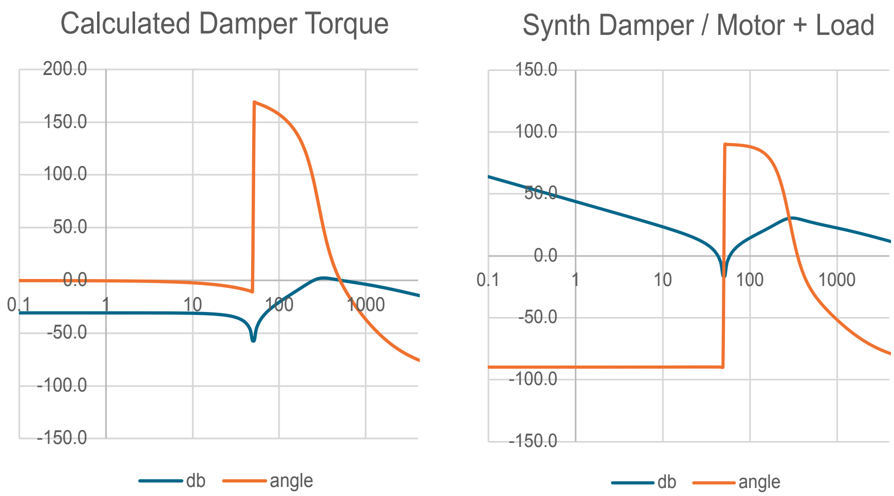

Figure 5—Synthetic inertial damper torque injection calculated from motor speed for motor plus shaft plus load inertia (left). Total system speed response to commanded torque including synthetic inertial damper torque injection (right). The system response to the synthetic inertial damper is shown equivalent to the response with a physical inertial damper.

The model works as the voltage source is modeled as a zero impedance, so the damper is essentially connected across Jm. Although this model is not realizable in a mechanical system, it does allow us to easily calculate the torque that a physical damper would incur if attached. While this model makes it easy to calculate the damper torque, it may be harder to picture how it works.

Another way to think about this model is to have the motor velocity (modeled as a voltage) drive the damper (Rd, Cd) with the same velocity (voltage) as the motor model. The torque (modeled as current) drawn by the damper is measured through Rd. This torque is subtracted from the original control torque It. The resultant net torque to the motor/shaft/load is identical to the torque that reaches the motor/shaft/load when a physical damper is in the system. Not surprisingly, the resulting system then produces the same response using the synthetic damper as it did with the physical damper!

In an actual system, this damping torque calculation would be done by measuring the actual motor position as the input, estimating the velocity, and calculating the equivalent synthetic inertial damper torque term. This damper torque term is then subtracted from the commanded torque (after some scaling for torque units used and for motor torque constant) to result in a very helpful improvement in the system dynamics. The actual system has some additional filtering terms to reduce the effects of encoder resolution with its stepwise output. These calculations are done in real time with minimized delay and are performed in the time domain, so they are a little more complicated than the simple impedance calculations in the spreadsheet, but they produce a very similar response.

Why Adding a Damper Improves Performance

In a basic system, the system gains, typically a position gain, velocity estimate (or simply derivative) gain, and integral gain, are limited by the gain/phase present in the physical system. A large inertia mismatch causes significant resonance peaking in the system. The velocity response of the system has a lag of 90 degrees as it is the integral of the acceleration. The position response of the system lags the velocity by 90 degrees as it is the integral of the velocity. This means if the motor and control system response were perfect, the position feedback would still be 180 degrees out of phase, meaning position-only gain would always be ready to oscillate (given enough gain to overcome friction). We add the velocity feedback to improve the phase margin of the system by anticipating when we will need to apply the brakes to avoid (or minimize) overshot. At just above the resonant frequency (about 510Hz for this model) of the motor/shaft/load without damper, we have a significant rise in gain to 64 db or about 1631, with a -90-degree phase, which means the gain must be set quite low to avoid having the system oscillate. With the damper added, however, the peak gain near the mechanical resonance has been reduced to 30 db (or about 33), while the phase at this maximum gain near resonance is 14 degrees positive rather than -90 for the motor velocity response. The system with a damper does not drop to a -45-degree angle until almost 754 Hz, a substantial improvement. Note that the non-damper system would need to have the gain significantly reduced (with the resulting bandwidth reduced) to avoid oscillating at the resonant frequency. The damper (either physical or synthetic) allows a much higher gain which also extends the bandwidth to allow for faster responses and much tighter control of a high inertia system. The phase boost also significantly helps even nominally low inertia systems and makes the tuning of the system much easier, often allowing the same tuning constants for an open shaft to five times motor inertia or larger with little change in the resulting motion when the load is varied.

Let's look at a couple of other example systems, starting with a geared or chain-fed system with backlash. These systems change their transfer function as the system is moving. That is, the load is only reflected to the motor when the teeth of the gear (or sprocket and chain) are in contact. When the motion reverses, the driving gear (sprocket) can rapidly accelerate while the teeth are disengaged (i.e., the load is decoupled). The teeth then slap, and according to the materials used, may significantly rebound. If the gain is high enough, or the load is positioned such that little torque is needed to keep it in position, a limit cycle oscillation may continue with the teeth bouncing off the adjacent teeth in both the clockwise and counterclockwise directions. This oscillation can quickly damage the gears while making much-undesired noise! When a physical damper is present, the inertia of the damper slows the acceleration of the decoupled motor. Upon contact between the teeth of the drive and load gears, the damper inertia continues at a higher rate than the motor for a short period, causing the teeth to not bounce off, or to have significantly less bounce, which allows the system to settle in without the limit-cycle oscillation. The damper effect allows the system gain to be significantly improved for better performance. The synthetic damper performs very similarly but without the added size and cost of a physical damper.

In some animatronic applications, for example, synthetic inertia can be made significantly larger than the physical motor inertia to help smooth out the motions in mechanisms having some degree of backlash. The damper then acts as a flywheel but with viscous damping. The flywheel action eliminates most of the high-speed vibrations which would otherwise make the motions look artificial.

In pumping applications, such as those involving a syringe-type pump, stiction may be a very significant problem. Stiction describes the fact that static friction is normally higher than dynamic friction, sometimes by a considerable degree. Stiction effects in a pump are noticed when the motion slows to a point where the seal on the moving piston begins to form mechanical bonds to the cylinder walls. This higher static friction coefficient may completely stop the piston until the control system can build up enough force to overcome the higher static friction coefficient, and then the piston lurches forward due to the lower dynamic friction coefficient. The resulting fluid flow is anything but smooth. The corrective action for this is to have sufficient gain and bandwidth in the system to rapidly adjust the forces so that the cylinder is not allowed to slow down. Rather, it can maintain the desired motion even in the presence of rapid variation in the frictional forces. Looking again at the physical damper, one might imagine a very stiff coupling grease and a large inertia that acts as a flywheel to prevent friction from stalling the motion. But this is only part of the solution, as the improved phase margin of the system with a (synthetic or physical) damper allows the gain to be significantly increased, allowing for both wider bandwidth and more powerful control system response to the friction variations, resulting in very smooth liquid dispensing even in the presence of stiction.

Note that the margins described here are just the plant torque to velocity forward transfer function wth a (synthetic) damper. Additonal installments will cover additional closed loop control techniques which are not available in a PID system which significantly benefit the performance of the improved control system.

PTE

quicksilvercontrols.com

Donald Labriola, P.E., is President of QuickSilver Controls Inc. (QCI), a producer of servo motors and controllers. Founded in 1996, QCI's genesis goes back to experiments in 1984 spinning hybrid step motors as servos motors. Labriola has vast experience in systems engineering and motion for medical applications and designing for UL CSA and regulatory testing.

Virtual End-of-Line Test—Prediction of the Acoustic Behavior of Gearboxes Based on Topographic Deviations Using Neural Networks

Marius Willecke, Dr. Jens Brimmers, and Prof. Christian Brecher

Tooth contact analysis is an integral part of the gear design process. With the help of these simulation tools, it is possible to calculate the excitation caused by a tooth contact (Ref. 1). Usually, the load-free transmission error or the total transmission error under load is used for this purpose. However, the calculation with the tooth contact analysis ZAKO3D allows only a quasi-static consideration of the excitation. To better evaluate the behavior in the overall system, it is therefore necessary to perform a dynamics simulation. However, the main disadvantage of such dynamics simulations is the much longer computing time compared to quasi-static tooth contact analyses due to the high computational effort.

In the context of measures such as the increase of resource efficiency as well as due to increasing demands of the end customers, the pressure on gearbox manufacturers to produce fewer rejects and at the same time to meet higher demands on the quality of the gearboxes is growing. To ensure that an assembled gearbox meets the acoustic requirements, tests are therefore carried out on the fully assembled units in end-of-line (EoL) tests (Ref. 2). If an anomaly is detected, the unit must be disassembled and overhauled as far as necessary or otherwise scrapped. It would be a significant advantage if assemblies, that are relevant for the acoustic behavior, such as the tooth meshes, could already be examined for their excitation behavior before assembling them.

Theoretically, this would be possible by simulating the acoustic behavior of the gearbox in a dynamics model, as it is currently used in the gear design process, using the real topographies of the gears to be installed. However, the main problem here is the calculation time of these dynamics models, which prevents a calculation parallel to the manufacturing process time.

To solve this challenge, a way must be found to predict the excitation behavior of the system much faster. One approach that is to be investigated for this purpose is the usage of metamodels, which allow a considerably faster calculation of the target variables. It is relevant here that a description of the tooth flanks is used, that is as exact as possible to be able to determine a realistic assessment of the excitation behavior that arises from the two wheels in the tooth mesh.

Willecke et al. (Ref. 3) have already shown that it is possible to use a substitute model for the quasistatic description of the problem. The approach developed there offers the potential to be used for dynamic calculations as well.

State of the Art

The work in this publication is mainly based on the preliminary work of Willecke et al. (Ref. 3). There is also an explanation of the structure and the application of deep neural networks (DNN) for the use of topographic deviations as input values. In the state of the art of this publication, generative adversarial networks (GAN) are explained.

Extending Datasets Through Generative Adversarial Networks

GANs are a subfield of Machine Learning and belong to the area of unsupervised learning. The basic idea is the use of two competitive DNNs. The two networks are a generator network and a discriminator network, see Figure 1. The generator network takes random input values and generates data from them. The discriminator network takes this generated "artificial" data as well as a set of "real" data. Based on patterns in the "real" data, the network tries to decide whether the "artificial" data is fake or real data. If the discriminator can recognize the generator's "artificial" data as such, the generator is informed about this and subsequently tries to generate more realistic data. If the discriminator is not able to recognize the "artificial" data of the generator as such, the discriminator is informed about it and improves itself afterward. This process continues until equilibrium occurs and the discriminator classifies p = 50 percent of the generated data as "artificial" and p = 50 percent of the generated data as "real" (Ref. 4).

Current challenges concerning GAN lie in achieving this converged state. Depending on the dataset, training method, and hyperparameters (see Figure 1), this is not always the case (Ref. 5).

GANs are often used in the generation or post-processing of images. Here, for example, based on a set of "real" images, new "artificial" images can be generated, or new "artificial" pixels can be created in an existing image, thus resharpening the image (Ref. 6).

Objective and Approach

The objective is to determine the characteristic values of the differential acceleration of a deviation-affected gear pair orders of magnitude faster than is possible with a conventional elastic multibody simulation model (EMBS) under load. Therefore, a DNN is developed that approximates the EMKS and achieves this time advantage. The method to be developed for calculating the characteristic values of the transmission error (TE) with this model is shown in Figure 2. It is assumed that each of the two gears is provided with a deviation. In the first step, these two deviation surfaces (AWF) of gear 1 and gear 2 are combined to a sum deviation surface (∑ AWF). Thus, an equivalent tooth contact is created in which only one gear has deviations, and the other gear has an ideal involute. In the second step, the parameter pi is derived from the ∑ AWF. These parameters should be able to describe the ∑ AWF as accurately as possible with as small of a number of control points as possible. In the third step, the parameter pi is given as input to the model, which then returns the TE characteristics.

Corresponding to the individual steps of the method for calculating the TE characteristic values for two gears with deviations, the procedure for achieving this goal can also be divided into several sub-steps. In the first substep, the ∑ AWF must be set up. For this purpose, the already developed procedure according to Willecke et al. based on the approach of Brimmers can be used (Refs. 3, 7).

In a third substep, the actual DNN for calculation is developed. For this purpose, a training data set with n = 3,000 data points is created. First, a pool of variants is generated. These are not combined fully factorially but distributed with the help of a Latin hypercube experimental design so that fewer variants are needed to cover the complete variation space. An EMBS calculation under load is performed with each variant of this variant pool. The acoustic parameters are then calculated for the differential accelerations calculated in this way. For each calculated variant of the pool, not only the parameters pi as input of the model are known, but also the acoustic parameters as output of the model. With the help of the data set created in this way, the DNN can be trained. A dataset created in analog with n = 480 data points, which are explicitly not part of the training dataset, is used to validate the created network.

Subsequently, it will be investigated how well the trained DNN is suited to predict data outside the trained range and how sensitive the network reacts to a reduction in the size of the training dataset. The GAN represents one way in which the dataset could be extended and refined for this purpose. The extent to which GANs can be used to selectively increase the size of the dataset for training is being investigated. The goal is to generate additional realistic training data.

Development of a Dynamic Model Considering the Topological Deviations in the Simulation of the Complete System

In this section, a model is set up with which the acoustic excitation of an e-drive transmission can be investigated for various topographical deviations. *Simpack* 2023 from Dassault Systems is used as the software

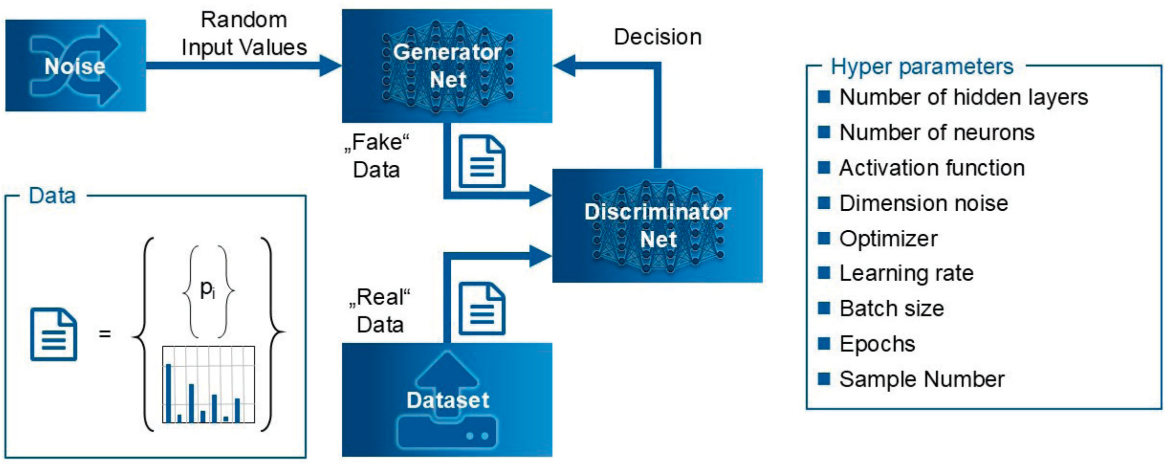

Figure 1—Structure of a generative adversarial network.

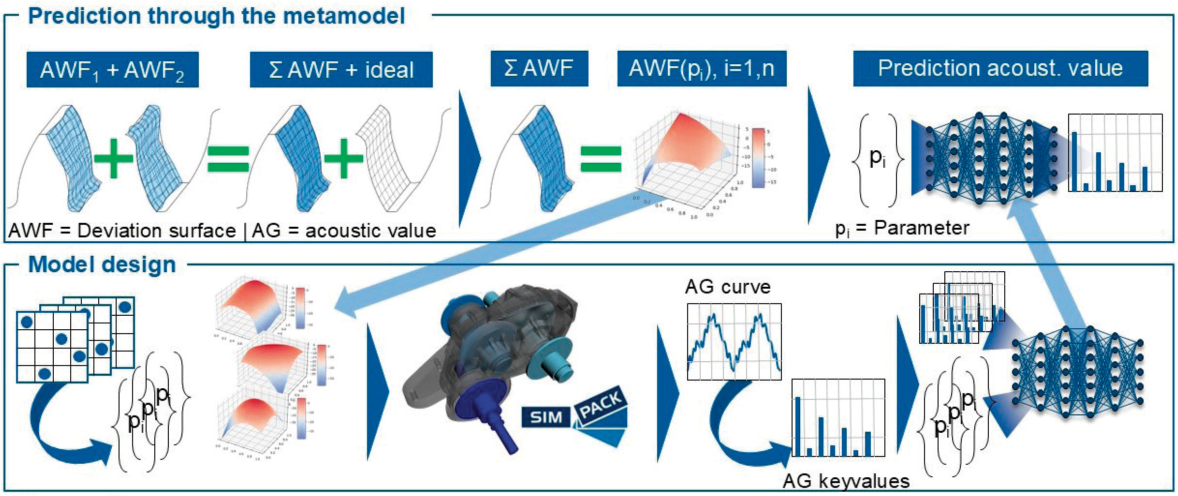

Picturesource: 3ds.com

Figure 2—Procedure for the construction of the deep neural network.

for the simulation environment. The exact use case is the high-speed demonstrator transmission of the WZL Gear Research Circle (Ref. 8). In the elaboration of this report, however, not both stages of the transmission are considered, but only the fast-rotating first stage. Experimental data on the test bench can be obtained for one stage as well as for two stages.

Modeling the Tooth Contact

The tooth meshing in the simulation model is modeled by the *Force Element 225: Gear Pair* (Ref. 9). The calculation method used is the DIN 3990 method B / Steiner approach. The number of slices in the width direction is limited to n_{Slices} = 5 for performance reasons (Ref. 9). The microgeometry can be specified in *Simpack* on the *Gear Pair* as a two-dimensional function of the amount of deviation over the tooth width and gear diameter. The deviation specifies the amount at the corresponding location that is removed from the ideal geometry. Negative values are not permitted. Therefore, no material can be added.

Modeling of Further Gearbox Components

In addition to the gearing, the other peripheral components of the transmission must also be modeled. These include all components that are in the power flow. The shafts, bearings, and housing as well as the fixation of the housing are considered here. The modeling of the corresponding components is described below. The structure is based on the structure of a dynamics model for a two-stage e-drive transmission described by Willecke et al. (Ref. 8).

Shaft and Housing

Both the shaft and the housing are prepared as modally reduced bodies. To create the modally reduced bodies, the geometries are exported as STEP files from the CAD model and imported into the CAE program *Abaqus* 2021, where they are meshed (Ref. 10). For this purpose, the shafts are manually partitioned to be able to use hexahedron-shaped elements in as large a volume as possible. These elements allow finer meshing with the same number of elements compared to tetrahedron-shaped elements. Thus, better results can be achieved with the same computing power. Beam models are not suitable for that use case hence they can't model the asymmetric modal behavior caused by keyways. However, due to the complexity of the housing, it will be meshed with tetrahedron-shaped elements. To ensure the quality of the meshing, a FE convergence study is performed, see Figure 3, left side.

If the edge length of the elements is reduced from l_k = 5 mm to l_k = 3 mm, the frequency of the first eigenmode changes by only Δf = 0.38 percent. It is thus assumed that with an edge length of l_k = 3 mm the modal behavior can be calculated with sufficient numerical stability. A further reduction of the edge length leads beyond the capacity of a node (RAM = 196 GB) of the used high-performance computer due to the resulting too-high number of elements, which cannot be solved any longer with the installed RAM. The modally reduced bodies are subsequently imported into *Simpack* and modeled there as linear flexible bodies. The eigenmodes are taken over from the calculation in *Abaqus*. Since all the components are still in the manufacturing stage, validation of the components modes was not yet possible. The model can later be updated with measuring data. This does not influence the following steps.

Bearings

The modeling of the bearings is done in *Simpack* with *Force Element 49: Bearinx Roller Bearing*. The force element is a user force extension of the company Schaeffler for *Simpack*. The bearings themselves are modeled in the Force Element based on maps. The maps were created by Schaeffler. The maps take the positions and velocities of the housing bore and the shaft as input and calculate the resulting reaction forces and torques.

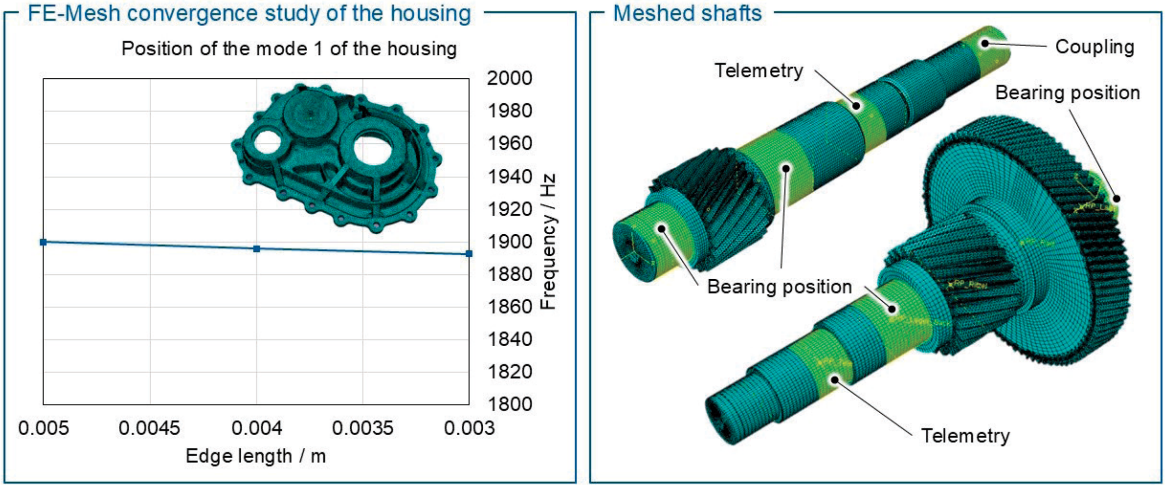

Figure 3—Mesh convergence study and networked components.

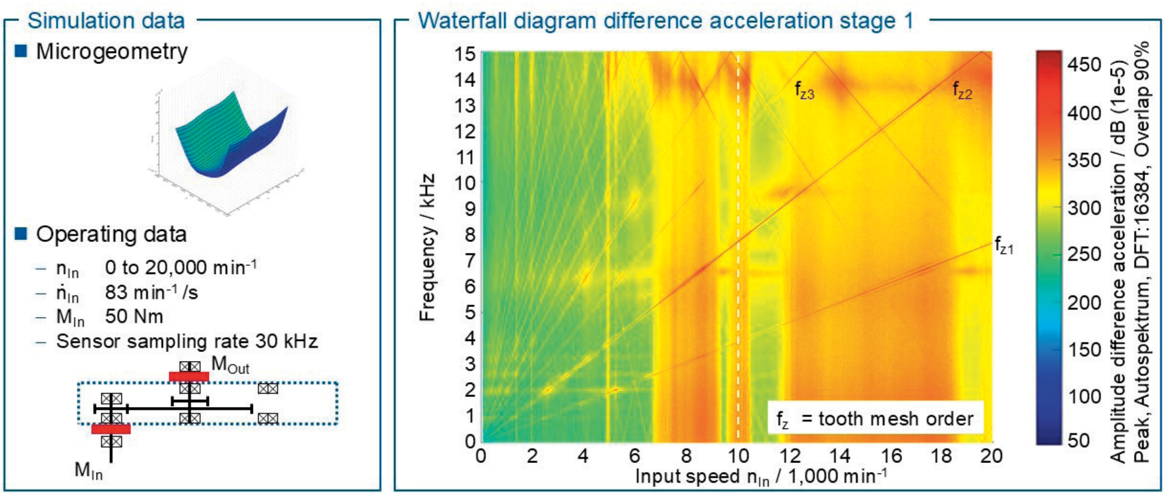

Figure 4—Calculated waterfall diagram of the gearbox up to n_{in} = 20,000 min^{-1}.

Assembling the Model

The individual components created are connected in *Simpack* by different *Force Elements* and thus assembled to form the overall model. The application of the torque is realized in two components. The first component applies tension with constant torque, which is balanced by the ratio of the transmission and thus does not lead to any acceleration of the drive train. The second component is imposed by a PI controller on the drive shaft. This controller adjusts the drive train to the specified speed curve. To drive the model efficiently, the control parameters of the controller must be set sensibly. To do this, the *P* component is first set to be minimally subcritical (K_p = 0.025) and then the I component is also set (K_I = 0.05).

The overall model created in this way can now be operated at any desired operating point. To obtain an overview of the behavior of the gearbox in the operating range, the gearbox is clamped at a torque of M_{in} = 50 Nm and then a pinion speed ramp-up from n_{in} = 0 min^{-1} to n_{in} = 20,000 min^{-1} is simulated. The calculated waterfall diagram of the speed ramp-up is shown on the right side of Figure 4. The placement of the two rotational acceleration measurement systems is marked in red on the left side of Figure 4. In the calculated waterfall diagram three significant areas can be seen where the tooth meshing frequencies go into resonance with natural frequencies of the overall system, resulting in increased response of the system. The speed n_{in} = 10,000 min^{-1} is selected as the operating point for further investigations, which is in the middle of the speed range of the gearbox. It is easy to see that this rotational speed lies in a range of increased resonance behavior of the gearbox and thus increased response of the system is to be expected at this operating point.

For further investigations, the simulations are now carried out at the operating point. Several phases are provided for moving the model cleanly from standstill to the operating point and performing measurements there. These are shown in Figure 5. In phase I from t_{model} = 0 s to t_{model} = 0.1 s, the load with which the

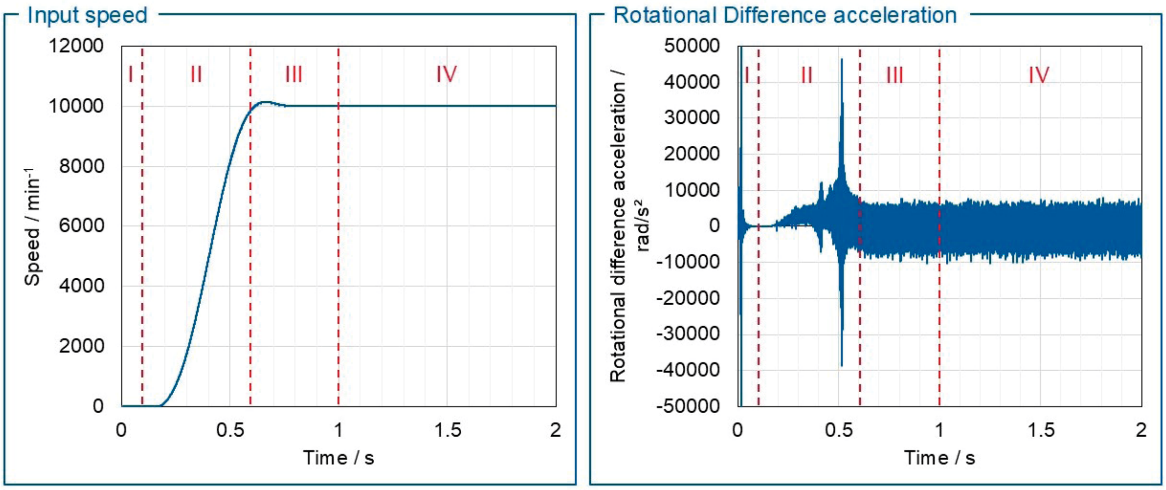

Figure 5—Time histories with sectors at the selected operating point.

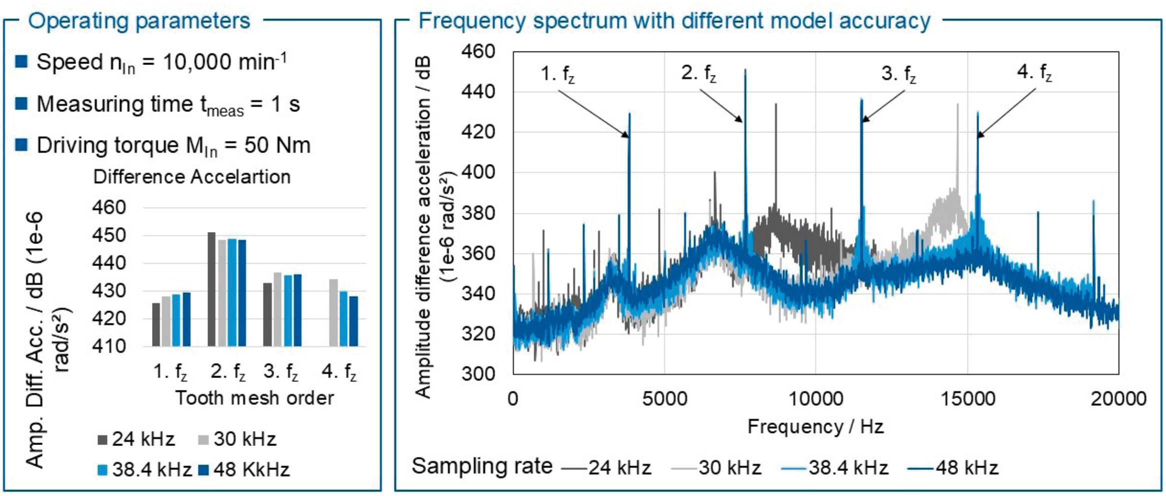

Figure 6—Influence of the considered modes on the system behavior.

system is braced is applied to the stationary system at a constant load change rate of $\dot{M}_{in}$ = 500 Nm/s. The load increases from M_{in} = 0 Nm to M_{in} = 50 Nm. The tension torque is constant in the further phases.

In phase II from t_{model} = 0.1 s to t_{model} = 0.6 s, the target drive speed n_{in},target, which is the setpoint of the PI controller, is increased with a constant target speed change rate of $\dot{n}$ = 20,000 min^{-1}/s. This results in a torque imprint by the controller that accelerates the model from rest from n_{in} = 0 min^{-1} to n_{in} = 10,000 min^{-1}. In phase III from t_{model} = 0.6 s to t_{model} = 1.0 s, no external variables are changed, and the model is given time to settle. In the course of the speed on the left side of Figure 5, the overshooting of the speed, caused by the discontinuity, in the acceleration specification can be seen well at the beginning of phase III. The model's behavior is stabilized in phase IV from t_{model} = 1.0 s to t_{model} = 2.0 s. The time course of this phase is used for the measurement, which is later used to calculate the acoustic characteristic values.

The eigenmodes of the flexible bodies were calculated up to a maximum eigenfrequency of $f_{eig,max}$ = 20 kHz to cover the entire human hearing range. However, since only the amplitudes of the tooth meshing orders are of interest for further evaluation, it is investigated whether modes can be removed to save calculation time without significantly changing the result. Therefore, at the intended operating point for the EoL, see Figure 6 top left, different sampling rates as well as maximum considered natural frequencies were investigated.

The right side of Figure 6 shows the frequency spectra at the selected operating point for four different sampling rates. The maximum considered natural frequency is in each case 0.42 times the sampling frequency to comply with the sampling theorem according to Shannon (Ref. 11). The amplitudes of the marked tooth meshing orders are shown separately in the bar chart at the bottom left of Figure 6 for better comparability. It can be seen well that at a sampling frequency of down to f_{sample} = 30 kHz there is no significant change in the amplitudes. No significant differences can be seen here in the entire frequency

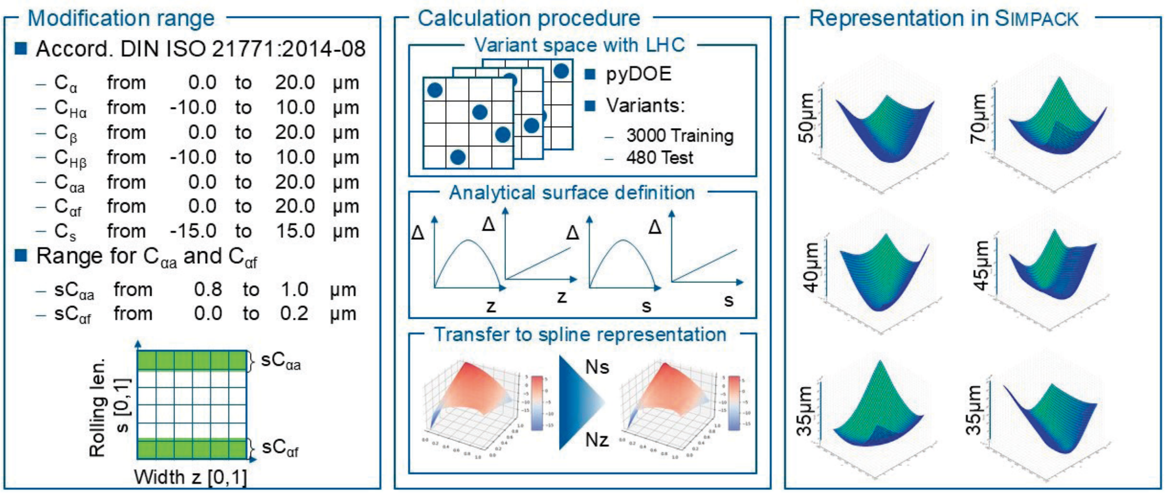

Figure 7—Modification range and application of the modifications in Simpack.

spectrum either. Only at a sampling frequency of f_{sample} = 24 kHz significant differences become visible. In the following, a sampling frequency of f_{sample} = 30 kHz and a maximum natural frequency of $f_{eig,max}$ = 12.5 kHz are used. The calculation time can thus be reduced from t_{sim} = 21.5 min to t_{sim} = 6 min by p = 72 percent.

Development of the Surrogate Model to Predict the Acoustic Characteristic Values

This chapter explains how the neural network is built. For this purpose, it is first described how the necessary data sets, which are later used for the generation and validation of the network, are generated. Furthermore, it is explained how the hyperparameters for the design of the network are selected. Subsequently, the validation of the prediction of the neural network is performed. For this purpose, the ability of the neural network to make predictions about previously unknown data is evaluated.

Variant Calculation with the Dynamic Model to Generate the Training and Test Dataset

The creation of the neural network, which is used as a surrogate model for the prediction of the acoustic parameters, requires a training data set. In addition, a test dataset is needed later for the validation of the prediction quality. Both data sets consist of different variants of topographic deviations. It should be noted that the variants of the test dataset are not part of the training dataset. The topographies are generated by free spline surfaces with N_z x N_s = 3 x 8 grid points out of analytical surfaces (Ref. 3). The procedure, see Figure 7 middle frame, is described by Willecke et al. (Ref. 3). To obtain freeform topographies as realistic as possible, they are generated from a superposition of standardized modifications (Ref. 3). According to Willecke et al. (Ref. 3), the range of these modifications is shown in Figure 7 on the left side.

The analytical surface is then converted into a free-form surface. This free-form surface is the topography that is subsequently used for the tooth mesh. To be able to imprint the topography on the *Gear Pair* in *Simpack*, it must be converted beforehand, see the section "Modelling the Tooth Contact." The right side of Figure 7 shows examples of some topographies and their processing in *Simpack*.

The data is transferred to *Simpack* as an "Input Function afs File" (Ref. 9). In this file the topography is stored with a resolution of 20 x 20 interpolation points. The intermediate points of the topography are mapped with a bivariate spline with two dimensions in both directions. A total of n_{var} = 3000 variants for the training data set and n_{var} = 480 variants for the test data set are generated with a Latin hypercube. The boundaries are designed to be wider than a possible occurring manufacturing deviation. The variants are subsequently simulated in *Simpack*. A variant of the training data set computes on average t_{sim} = 965.16 s and a variant of the test data set computes on average t_{sim} = 943.67 s. The generation of the training data set thus takes t_{sim} = 2,895,480 s, which corresponds to d = 33.5 days of computing time, and the generation of the test data set requires t_{sim} = 463,277 s, which corresponds to d = 5.24 days of computing time. However, the calculations can be performed in parallel, so that the real time required can be reduced by the factor of the parallel calculations if the corresponding IT infrastructure is available.

The scatter of the simulation time of the individual variants in the data sets is shown on the left side of Figure 8. All calculations are performed as single-core calculations on a workstation (CPU: i7-8700 / 64GB Ram).

However, n_{par} = 10 variants are calculated simultaneously, since the time the user has to wait for the results can be reduced efficiently this way. After the variant calculation is completed, the differential acceleration between t_{model} = 1 s and t_{model} = 2 s in the time domain is calculated for each variant. This time signal forms the basis for the calculation of the acoustic parameters. The characteristic values are used, whose applicability Willecke et al. could already

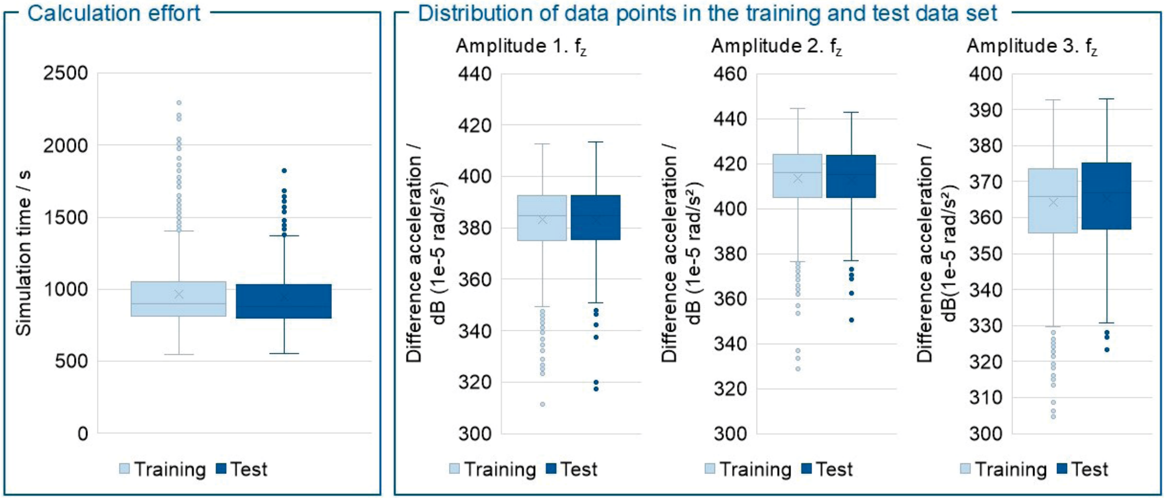

Figure 8—Distribution of acoustic parameters in the training and test data set.

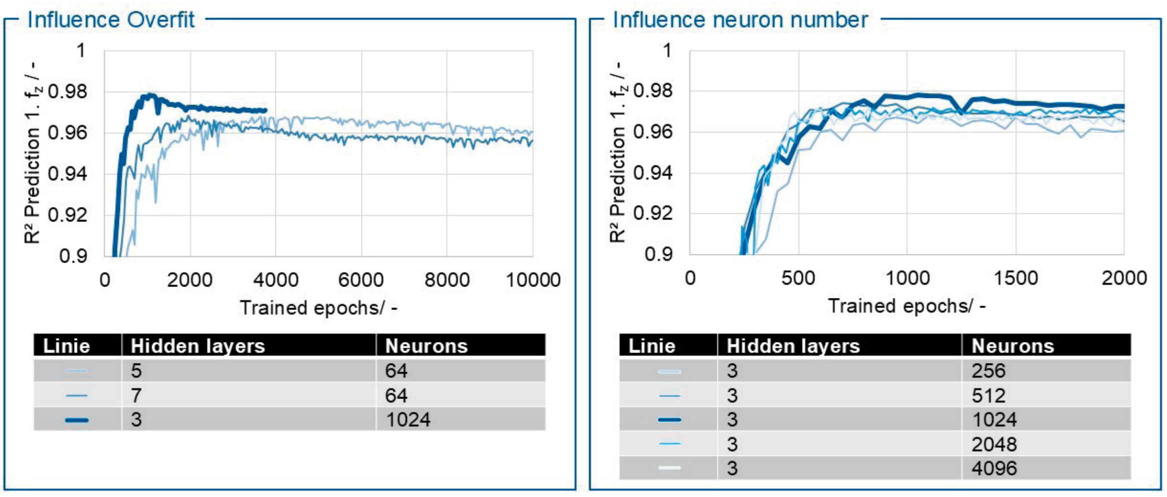

Figure 9—Effect of overfitting and influence of neuron number.

prove in the quasistatic tooth contact analysis (Refs. 3, 12).

In the following, the amplitudes of the first three tooth meshing orders are used for the elaboration. The distribution of the amplitudes of the individual tooth meshing orders over the variants is shown on the right side of Figure 8. It is easy to see that the amplitudes of most variants move in a narrower band and there are only a few outliers in the low amplitude range. The position of the mean values and quartiles for the training and test data set is similarly distributed, so that it can be assumed that the test data set is also representative of the area of the network for which the training data set provides input values.

Optimal Choice of Hyper-Parameters for the Neural Network

The neural network is characterized by various parameters. These parameters, which are basically the settings of the network, are called hyperparameters. To find a starting point for the selection of the hyperparameters, first the same was chosen, which led to good results in a network for the prediction of the characteristic values of a quasistatic tooth contact analysis (Ref. 3). A square-error function was used here since it is suitable for regression problems (Ref. 13). As learning rate l = 0.0001 is used. The network thus learns more slowly but achieves a higher quality (Ref. 3). The softplus function is used as the activation function in the hidden layers since it has proven to be particularly useful for the problem (Ref. 3). The number of hidden layers as well as the number of neurons per layer will be adjusted for this model. The training is done with a group size of $s = 32$ (Ref. 3).

A problem in training neural networks can be the overfit of the network to the data of the training data set. To investigate the occurrence of this effect, the network is trained with the training data set for a few epochs and then tested to determine the quality with which the test data set can be predicted. The quality of the prediction is defined by the coefficient of determination (R^2 value). On the left side of Figure 9, the course of the R^2 value for the prediction of

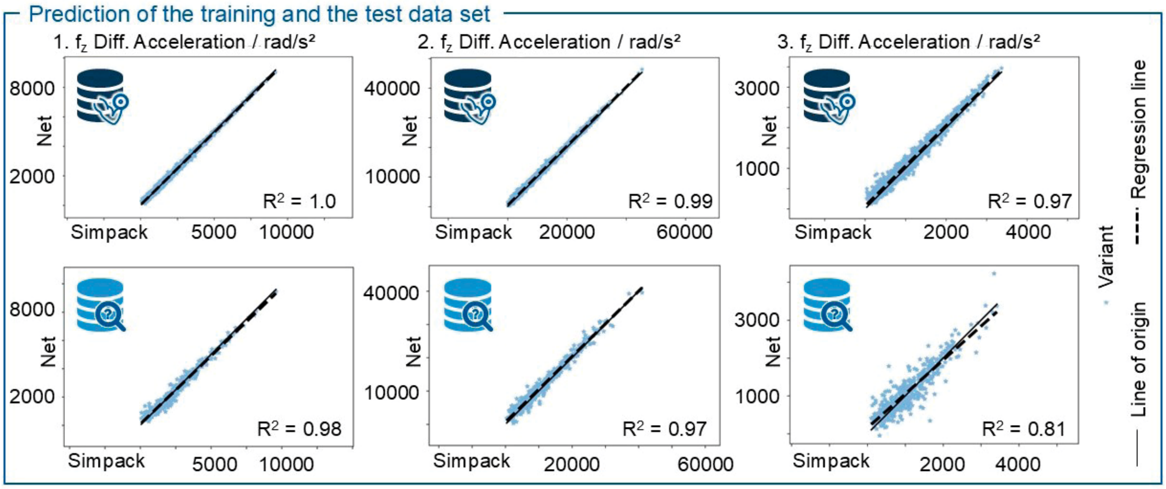

Figure 10—Prediction of the training and the test data set.

the first tooth meshing order of the differential acceleration is shown for three network topologies.

It is easy to see that the R^2 value first increases rapidly and then slowly decreases again after it has reached a maximum. The position of the maximum depends on the number of neurons and the number of hidden layers. The investigations of Willecke et al. on quasi-statics as well as the evaluation of the data set of the dynamics of the model investigated here show that three hidden layers lead to the best prediction quality in principle (Ref. 3). To investigate how the number of neurons in the hidden layers affects the quality of prediction, it is varied for training dataset. The results of the variation are shown on the right side of Figure 9. It can be seen well that a neuron count of n_z = 1,024 leads to a better R^2 value than the other network topologies. Therefore, in the following, a network topology consisting of three hidden layers with n_z = 1,024 neurons is used.

Validating the Model with a Test Dataset

The DNN is built up and trained with the hyperparameters defined in the section "Optimal Choice of Hyper-Parameters for the Neural Network." The network is used in the training state, which has just no overfit and lies in the maximum of the prediction quality, see Figure 9 on the left. To check the prediction quality, the data points of the test data set are predicted with the trained network. Subsequently, the predicted acoustic characteristic values are compared with the calculated acoustic characteristic values. This is shown in Figure 10 for the first, second and third tooth meshing order of the differential rotational acceleration.

The first row of the diagrams shows the prediction of the training data. It is easy to see that all variants lie very well on the line of origin in the diagram, i.e., the predicted values correspond almost without deviations from the originally calculated values. This also results in coefficients of determination $R^2 \approx 1$. The second row of the diagrams shows the prediction of the variants of the training data set. Again, the points of the individual variants for the first two fz are very close to the line of origin and the R^2 values indicate a good mapping of the data set. Only the prediction of the amplitudes of the third tooth meshing order shows larger deviations and thus also only fulfills a value of R^2 = 0.81. The prediction of the entire test data set thereby takes t_{sim} = 0.057 s in comparison to t_{sim} = 463 277 s in the EMBS model, see the section "Optimal Choice of Hyperparameters for the Neural Network." Thus, the prediction by the network is faster by a factor of ΔDNN = 8 127 666.

Investigating the Influence of the Number of Data Points in the Training Data Set

The number of data points in the training dataset used to create the neural network has an impact on the prediction quality achieved by the network. To investigate this influence, the number of data points used from the training data set to create the DNN is varied. For this investigation, a random sample of data points is taken from the entire training data set and the DNN is only trained with these points. To exclude the possibility of an influence due to the specific chosen random points, the process is repeated n = 15 times for each data set size and the mean value and standard deviation of the achieved prediction quality are calculated. For the network, the same topology and the same hyper-parameters are used, which were worked out in the section "Optimal Choice of Hyper-Parameters for the Neural Network." The results are shown in Figure 11.

It is easy to see that with an increasing number of training data points, the quality of the prediction increases rapidly at the beginning and increases much more slowly with an increasing number of data points. However, the effort to generate the data points increases linearly, since for each data point in the training dataset an equally effortful simulation must be performed.

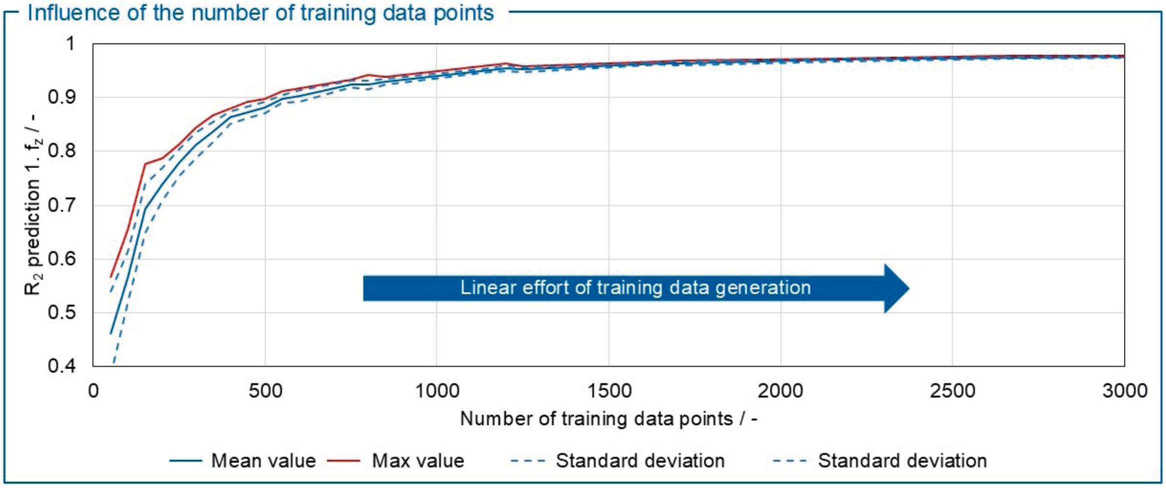

Figure 11—Influence of the number of training data points on the prediction quality.

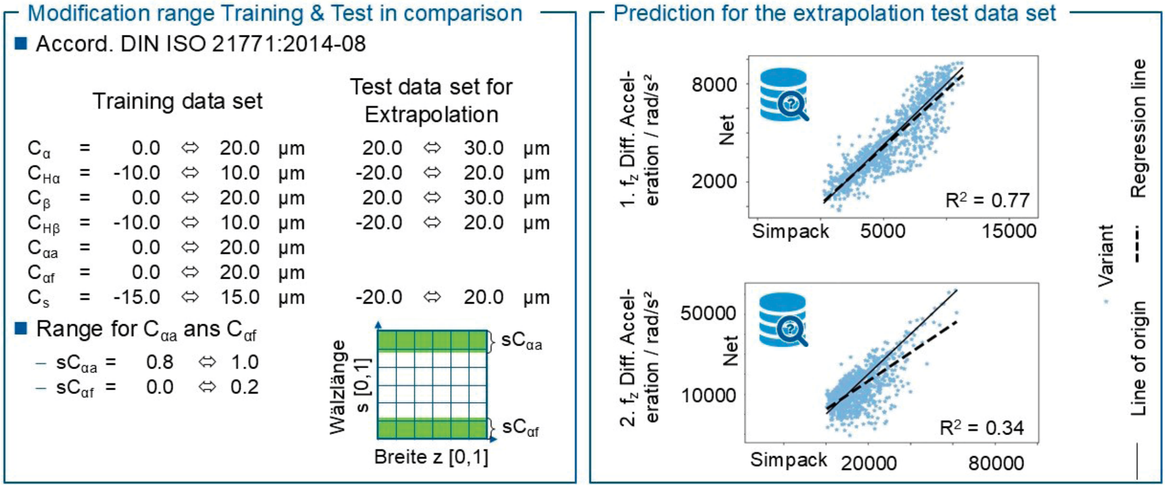

Figure 12—Range of variation and prediction quality for the extrapolation test data set.

Investigation of the Extrapolation Capability of the Neural Network

The behavior of the neural network has so far only been tested and evaluated in the range for which it has been explicitly trained. To investigate how the network behaves outside this range, a further test data set with n = 1,000 variants is created. The deviations of this data set are shown in Figure 12 on the left.

They extend beyond the boundaries of the training data set so that the mesh is forced to extrapolate. The right side of Figure 12 shows the prediction of the amplitude of the first and second tooth meshing frequencies of the differential rotational acceleration of the extrapolation test data set. For the first tooth meshing order, a principal grouping of the values around the origin line can still be seen. However, the R^2 value of $R^2 = 0.77$ indicates that the prediction of the extrapolated data is of low quality. The prediction of the second tooth meshing order shows only a R^2 value of $R^2 =$ 0.34. Here it is clearly visible that no meaningful prediction can be made with the developed approach. The DNN can therefore only be used for extrapolating predictions to a very limited extent.

Extending the Training Data Set with the Help of a Generative Adversarial Network

The section "Investigating the Influence of the Number of Data Points in the Training Data Set" shows that a training data set with a too-small number of training data points leads to a DNN with a worse prediction quality. Furthermore, it is shown in the section "Investigation of the Extrapolation Capability of the Neural Network" that the DNN also has a lower prediction quality for predictions that go beyond the boundaries of the trained domain. The first challenge, that a too-low prediction quality is achieved with too few training data points, can be met trivially by using more training points. The second challenge can be met by increasing the size of the training domain itself. However, this decreases the density of data points in the trained domain, so the number of training data points must also

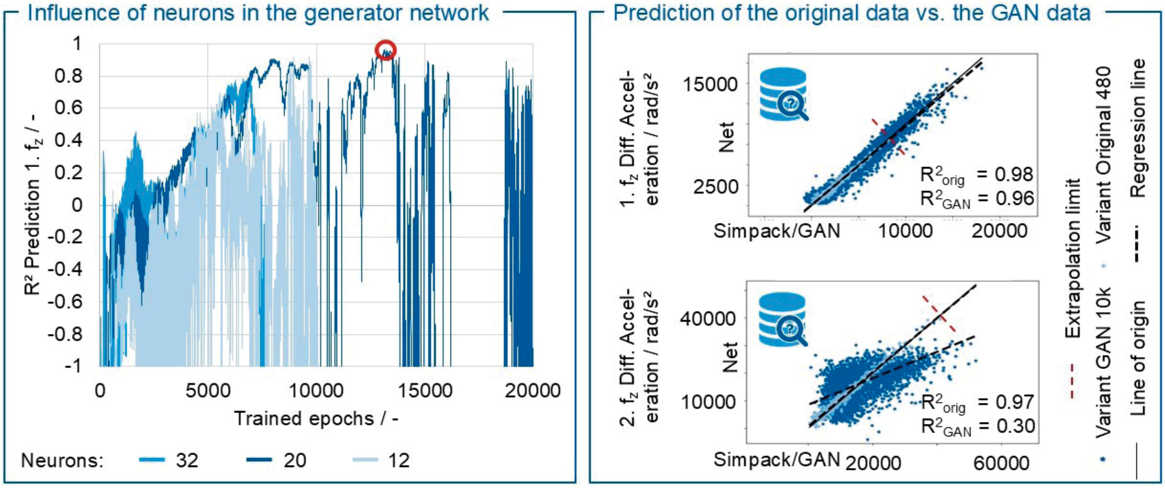

Figure 13—Influence of generator network neurons on data generation with the GAN.

be increased. A major disadvantage of generating a larger training dataset is that, classically, more simulations must be performed with the EMBS model. This is very computationally expensive.

An alternative to generating more data when an initial data set is already available can be a GAN, see the "State of the Art" section. These networks are typically used to create new data that fits the pattern of existing data. The resulting augmented dataset can then in turn be used as a training dataset for the DNN. Classical GANs are usually designed to process images (Ref. 6). The data here has the size of the number of pixels in the height direction times the number of pixels in the width direction times the number of color values per pixel.

However, the data in the use case to be investigated here is a vector with 18 grid points of the topography as input and a vector with the acoustic characteristic values of the corresponding variant as output values. GANs try to recognize patterns in existing data and generate new "artificial" data based on these patterns. Therefore, the input variables of the grid points and the output variables of the characteristic values must first be converted into a suitable format. For this purpose, the input and output vectors are stacked on top of each other to a new vector, see Figure 1, so that a data set is created that no longer consists of pairs of input and output quantities, but only of a single vector per data point. The GAN can now attempt to generate new "artificial" vectors based on the existing vectors as "real" data.

As a test for the applicability of a GAN the data set with n = 480 points is used, see section "Variant Calculation with the Dynamic Model to Generate the Training and Test Dataset." If the DNN, which is used for prediction, is trained with only n = 480 points, the quality of the prediction is not sufficient, see section "Investigating the Influence of the Number of Data Points in the Training Data Set." The goal is therefore to enlarge the data set consisting of n = 480 points with a GAN in such a way that a new DNN can be trained with it, which then provides improved prediction accuracy. The correct choice of hyper-parameters has a significant influence on the results of the GAN (Ref. 5). These hyper-parameters are therefore investigated in the following.

To verify whether the GAN provides meaningful results, the generated data must be examined. When "artificial" images are generated, they can be viewed by a human and it is obvious to the human whether they look realistic or not. This is not the case with the generation of "artificial" vectors. Therefore, the "artificial" vectors are again decomposed into input and output variables and then predicted using the DNN from the section "Validating the Model with a Test Dataset." Based on the validation in the section "Validating the Model with a Test Dataset," it is assumed that the DNN correctly represents the model behavior. Thus, if the "artificial" points generated by the GAN can be correctly predicted by the DNN, it can be assumed in principle that the GAN works. The quality of this prediction is again evaluated with the R^2 value. On the left side of Figure 13 the influence of different numbers of neurons in the generator network is shown.

It can be seen well that in the first n = 10 000 epochs the R^2 value of the "artificial" data increases. However, discontinuities occur afterward and there seems to be no convergence of the GAN. In principle, however, a neuron number of $n_{Neur,Gen}$ = 20 seems to provide the most promising results. For the data set from this GAN, which reaches the highest R^2 value (red circle on the left side of Figure 13), a comparison between the original data set and the "artificial" GAN data is shown on the right side of Figure 13. It is particularly noticeable that only the points of the first tooth meshing frequency are apparently correct. Furthermore, it is noticeable that the value range of the GAN data extends beyond the value range of the original data. If one now considers the fact, that the DNN, which is used as the basis for calculating the R^2 value, has a lower quality for extrapolating statements, the assessment of the quality of the

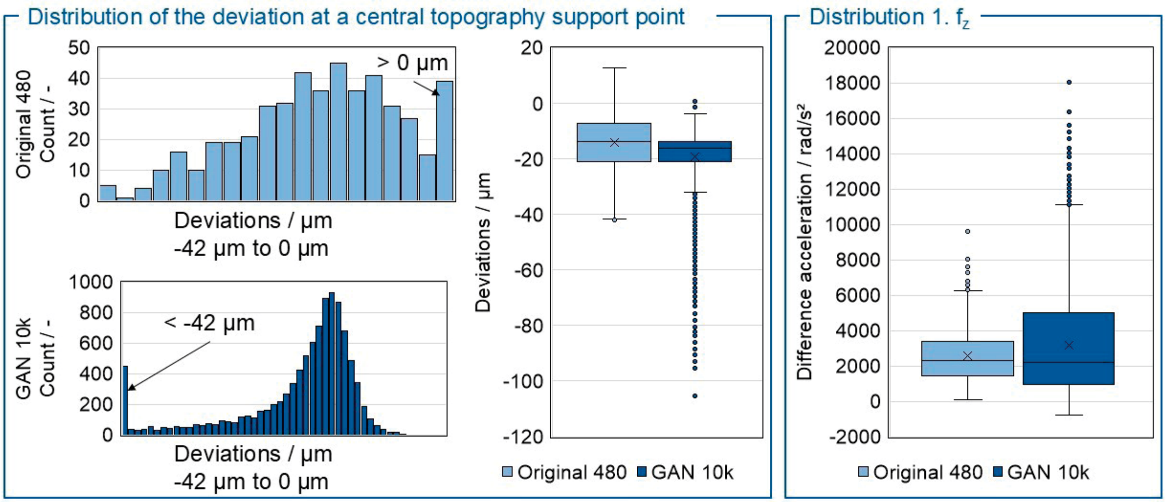

Figure 14—Comparison of the value ranges of the original and the GAN data set.

data generated by the GAN must be questioned here. The aspect of plausibility is further examined in Figure 14. Here, the distributions of the deviation values at a point in the center of the topography are shown in comparison on the left side as an example. From the distribution shapes as histograms, principal differences in the data sets can be recognized. If the original data set also shows deviations greater than Δ_{topo} = 0 µm at the point under consideration, the GAN data set instead shows values smaller than Δ_{topo} = 42 µm. In the boxplot diagram to the right of the histograms, this scatter is also illustrated.

The right side of Figure 14 shows the distribution of the first tooth meshing frequency as a result of values for both data sets side by side. Here it can be seen well that although the input variables seem to be concentrated in a narrower range, the result variables scatter over a wider range. After optimizing the hyper-parameters of the generator network, the hyper-parameters of the discriminator network are optimized. Hereby the R^2 value of the GAN data, related to the DNN from the section "Validating the Model with a Test Dataset," can be improved again to R^2 = 0.995. However, many data points still lie outside the range of values defined by the "real" data. If one removes all data points newly generated by the GAN, which would represent an extrapolation, then the R^2 value of the remaining generated points decreases. The remaining "artificial" points are then added to the initial data set of n = 480 "real" points. Thus, a new DNN is generated analogous to the section "Investigating the Influence of the Number of Data Points in the Training Data Set." However, the newly generated DNN has the same prediction quality as the network consisting of the n = 480 "real" points alone, cf. Figure 10. The additional "artificial" data have therefore not yet improved the prediction of the DNN. However, the "artificial" data also did not worsen the prediction of the DNN either, so that in principle functionality of the GAN can be assumed. To achieve the desired added value with the GAN, further research is necessary.

Summary and Outlook

Within the scope of this work, an EMBS model for the first stage of a two-stage gearbox was built in the *Simpack* simulation environment. The high-speed demonstrator gearbox of the WZL Gear Research Circle was chosen as the application case. During modeling, attention was paid to a high-performance design of the model. Structural components are integrated as modally reduced bodies. To ensure convergence in the modal reduction, an FE study was carried out. Furthermore, a simulation study on the influence of the maximum considered eigenmodes in combination with the maximum necessary sampling frequency was carried out in the built EMBS model. The settings were optimized in such a way that a minimum calculation time could be achieved without accepting significant deviations in the calculation of the acoustic parameters. The microgeometry of the gears was imported into the model as topography via Input Functions of *Simpack*. To analyze the operating point for the following simulations, a run-up was calculated and evaluated in a waterfall diagram. With the simulation model optimized in this way, two variant calculations were carried out at the operating point. One with n = 3,000 variants to generate the training data set for the neural network and one with n = 480 variants to generate the test data set. The points in both data sets were distributed with a Latin Hypercube. Based on the preliminary work of Willecke et al. the basic structure of the DNN was chosen for the construction of the network developed in this work (Ref. 3). Subsequently, an optimization of the hyper-parameters was carried out for the network to achieve an optimal prediction quality. A coefficient of determination of R^2 = 0.98 was achieved for the test data set. In the prediction of the test data set, a speed advantage by a factor of Δ_{DNN} = 8,127,666 was achieved. This speed advantage makes it possible to predict the excitation behavior of the gearbox based on the topography in parallel with the process time of manufacturing. The objective is therefore fulfilled.

An essential prerequisite for the generation of the DNN, which is used for the prediction, is a sufficiently large training data set. Generating sufficiently large data sets can take a significant amount of time. To be able to generate a sufficiently large training data set with fewer data points, the usability of GAN was investigated. It could be shown that a GAN is in principle capable of generating data points similar to those contained in the reference data set. However, stable convergence could not be achieved with the GAN yet. Likewise, the generated data could not yet improve the prediction network. Further investigations are necessary until the GANs can be used for the described application. For this, further hyper-parameter studies are essential on the one hand; on the other hand, the learning and evaluation method of the GAN can still be optimized so that nongradient-based methods are used.

PTE

Marius Willecke, M. Sc. studied Mechanical Engineering at RWTH Aachen University 2019, graduating with distinctions. Since 2019, he has served as a research assistant at WZL of RWTH Aachen University. His primary interests include end-of-line testing development of tooth contact simulation software and simulation of the acoustic behavior of gearboxes.

Dr.-Ing. Jens Brimmers is the head of the gear department at the Laboratory for Machine Tools and Production Engineering (WZL) of RWTH Aachen University since June 2019. He graduated from RWTH Aachen University with master's degrees in mechanical engineering and business administration. His Ph.D. thesis focused on beveloid gears and topological tooth flank modification.

Prof. Dr.-Ing. Christian Brecher has been, since January 2004, Ordinary Professor for Machine Tools at the Laboratory for Machine Tools and Production Engineering (WZL) of the RWTH Aachen, as well as Director of the Department for Production Machines at the Fraunhofer Institute for Production Technology IPT.

Bibliography

1. Hemmelmann J. E., 2007, "Simulation des lastfreien und belasteten Zahneingriffs zur Analyse der Drehübertragung von Zahnradgetrieben," Diss., Werkzeugmaschinenlabor (WZL) der RWTH Aachen, RWTH Aachen University, Aachen. Eng. Title: Simulation of load-free and loaded gear meshing for analysis of rotary transmission of gear trains.
2. Berger V., Wilbertz A., and Meyer I., 2010, "Körperschall Im End-Of-Line-Test Von Doppelkupplungsgetrieben," ATZproduction(3), pp. 24–27. Eng. Title: Structure-borne noise in the end-of-line test of dual clutch transmissions.
3. Willecke M., Brimmers J., and Brecher C., 2023, "Surrogate model-based prediction of transmission error characteristics based on generalized topography deviations," Forschung im Ingenieurwesen.
4. Brownlee J., 2019, "A Gentle Introduction to Generative Adversarial Networks (GANs)," *https://machinelearningmastery.com/what-are-generative-adversarial-networks-gans/*.
5. Mescheder L., Geiger A., and Nowozin S., 2018, "Which Training Methods for GANs do actually Converge?," International Conference on Machine Learning.
6. Goodfellow I., 2016, "NIPS 2016 Tutorial: Generative Adversarial Networks," NeurIPS | 2016: Thirtieth Conference on Neural Information Processing Systems.
7. Brimmers J., 2020, "Funktionsorientierte Auslegung topologischer Zahnflankenmodifikationen für Beveloidverzahnungen," Diss., RWTH Aachen University, Aachen. Eng. Title: Function-oriented design of topological tooth flank modifications for beveloid gears.
8. Willecke M., Brimmers J., and Brecher C., 2022, "Evaluating the Capability of Acoustic Characteristic Values for Accessing the Gearbox Quality," 13th Aachen Acoustics Colloquium 2022, 1st ed., Aachen Acoustics Colloquium GbR, Aachen, pp. 125–134.
9. SIMPACK GmbH, 2020, "*SIMPACK* 2020x Documentation," Firmenschr., SIMPACK GmbH.
10. Dassault Systèmes, 2011, "*Abaqus 6.11: Abaqus*/CAE User's Manual," Bed.-Anl., Providence, RI, USA.
11. Shannon C. E., 1948, "A Mathematical Theory of Communication," Bell Sys. Tech. J. (27), pp. 623–656.
12. Willecke M., Brimmers J., and Brecher C., 2021, "Virtual Single Flank Testing—Applications for Industry 4.0," Procedia CIRP, 104, pp. 476–481.
13. Ketkar N., 2017. Deep Learning with Python: A Hands-On Introduction, Apress L. P, Berkeley, CA.

TIMKEN

Appoints New President and Completes CGI Acquisition

The Timken Company recently appointed Tarak Mehta the company's president and CEO. Mehta was also elected to Timken's board of directors.

"I'm excited to join Timken and hear directly from our employees, customers and other stakeholders all around the globe about how we can accelerate profitable growth and continue to drive momentum for the company," said Mehta. "I look forward to collaborating with our talented team to identify additional opportunities to advance customer-centric innovation."

Following a comprehensive search process, the Timken board of directors announced in March that Mehta, who previously served as a member of ABB's group executive committee and president of its Motion business, would succeed Richard G. Kyle as president and CEO. Mehta spent 26 years at ABB, a $32 billion leader in electrification and automation. He is an accomplished strategic leader with a proven record of delivering results, developing global teams and achieving operational excellence.

Mehta succeeds Kyle, who has moved into an advisory role to assist with the leadership transition after 10 years as CEO. Following the transition, Kyle plans to retire as a Timken employee in February 2025 but will continue to serve on the company's board of directors.

"On behalf of the Timken board of directors, I want to commend Rich for his contributions and leadership during a decade of strong growth and transformation for the company," said Timken Chairman John M. Timken Jr. "As we look to the future, Tarak brings the deep experience and expertise we need to continue to advance our strategy and build on our 125-year legacy. Based on his impressive track record and strong business acumen, we're confident that Tarak is the right leader to guide us through our next chapter of profitable growth."

Additionally, Timken has completed its previously announced acquisition of CGI, Inc., a Nevada-based manufacturer of precision drive systems serving a broad range of automation markets with a concentration in medical robotics.

"Timken has one of the broadest and most differentiated precision drive product portfolios in the global automation industry," said Christopher Coughlin, executive vice president and president of Industrial Motion. "Driven by our strength in operational excellence, growing global footprint and expanding engineering expertise, we are well positioned for growth in attractive markets such as medical, solar, factory automation, aerospace, general industrial and more."

"CGI's precision motion-control offerings closely complement our Cone Drive harmonic and Spinea cycloidal products. With an attractive product portfolio, strong presence in high-growth medical applications, state-of-the-art manufacturing and consistently strong operating margins, the CGI acquisition is a good strategic fit for Timken that will help us continue to build on our 125-year legacy of innovation," continued Coughlin.

Timken entered the precision drives space in 2018 by acquiring Cone Drive and expanded its capabilities in 2022 by adding Spinea. These acquisitions were a direct result of Timken's strategy to diversify and expand its capabilities in industrial motion. Cone Drive and Spinea solutions enable a wide range of applications and are helping to drive Timken's growth in automation, which ranked as the company's second-largest individual end-market sector in 2023. The addition of CGI will further bolster Timken's position as a global leader in automation and robotic solutions.

CGI is a family-owned business founded in 1967 with headquarters and production facilities in Carson City, Nevada. The company employs approximately 130 people and is expected to generate around $45 million in sales in 2024.

cgimotion.com
timken.com

FOREST CITY GEAR

Celebrates Amy Sovina's 30th Anniversary

Forest City Gear, a manufacturer of fine- and medium-pitch custom gears, proudly recognized Amy Sovina on her 30th anniversary and thanked her for her long-term dedication to the company.

Sovina is Forest City Gear's quality assurance manager, responsible for managing gear inspection, implementing quality policies and procedures, coordinating audits, and safeguarding accreditation statuses. Sovina is well-respected for her knowledge and mentorship, both internally and externally.

"It has been a joy to watch Amy grow her skills throughout the last 10 years," says Jeff Mains, director of technical operations. "She has grown more confident with her communication skills with other employees and with our major OEM customers. This has allowed her to excel to new opportunities within FCG. She's a fast learner, and she enjoys challenges—especially on the golf course."

forestcitygear.com

January 7–10

CES 2025

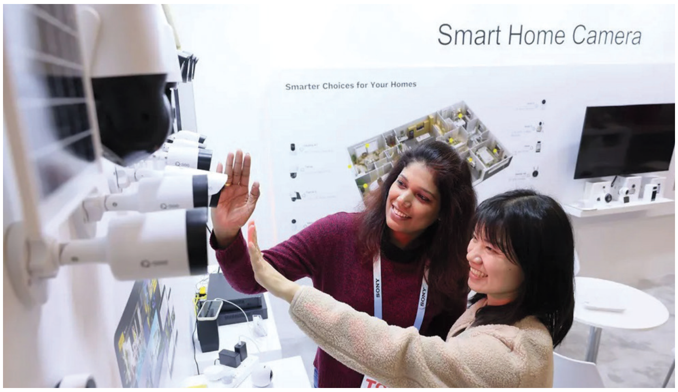

Attracting a diverse range of professionals, including executives, engineers, designers, and entrepreneurs, CES (Las Vegas) is an excellent opportunity to connect, collaborate, and grow your professional network. Keynote addresses and panel discussions from industry experts offer valuable insights into market trends, consumer behavior, and emerging technologies that can help guide strategic decisions and future planning. Attendees can interact with new technologies firsthand, gaining a deeper understanding of their features and potential applications. The broad range of exhibits and industries represented at the show can inspire innovative solutions. Industries include 3D printing, AR/VR/XR, AI, cloud computing/data, construction tech, cybersecurity and more.

powertransmission.com/events/992-ces-2025

February 4–6

Additive Manufacturing Strategies 2025

The Additive Manufacturing Strategies conference (New York) brings together AM stakeholders from all over the world. AMS includes panels and keynotes on topics most critical in the fast-growing world of additive manufacturing. Bringing together the industry's leaders in a contained networking environment makes AMS the place for startups to access capital, for financial institutions and investors to sharpen their radars, and for the AM industry to focus on the business of AM. AMS 2025 is "in-person only" to ensure maximum networking and discussion.

powertransmission.com/events/990-additive-manufacturing-strategies-2025

February 11–13

PowerGen International 2025

PowerGen (Dallas) is the largest network and business hub for electricity generators and solution providers engaged in power generation. Power producers, utilities, EPCs, consultants, OEMs, and large-scale energy users gather at PowerGen International to discover new solutions as large, centralized power generation business models evolve into cleaner and more sustainable energy sources. This year-round platform of digital education, current and breaking industry news, thought leadership articles, quality matched meetings, and industry-leading live events provide a hub for power generation professionals to learn and network.

powertransmission.com/events/909-powergen-international-2025

February 11–13

Industrial IoT Conference 2025

The Industrial IoT Conference (Ft. Lauderdale, FL) explores the potential of intelligent machines, prescriptive analytics, sensor driven analytics, and block chain solutions. Attendees learn about the industrial IoT technologies that are driving the transformation in manufacturing, supply chain and operations. Attendees include implementors, manufacturing companies, supply chain professionals, service providers, IoT manufacturers and more. Topics include implementation, warehouse logistics, robotics, sensors, cybersecurity, data analytics and more.

powertransmission.com/events/972-industrial-iot-conference-2025

February 18–20

MDSM 2025

Motor, Drive Systems and Magnetics (MDSM), Tallahassee, FL., features the latest technical advancements in motor, drive systems, motion control, magnetic applications, technology, and rare earth materials. This is an opportunity for professionals to hear content in design, efficiency, and application advancements in automation, robotics, manufacturing, utilities, automotive, medical, consumer, aerospace & defense industries. Motor & Drive Systems is focused on the latest technical advancements impacting the design, integration, and efficiency of motor, drive systems, and motion control.

powertransmission.com/events/966-mdsm-2025

AD INDEX

CALL FOR PAPERS!

Are you sitting on an idea for a technical paper but wondering where to present it? Do you have one already written, sitting on your desk, gathering machine dust?

How about *Power Transmission Engineering*? We are always looking for gearing- and power transmission component-relevant technical papers for publication in the magazine and in its digital version. Having your work appear in *Power Transmission Engineering* guarantees you an audience of the most experienced and discriminating industry players. You say your work has not been peer-reviewed? Not a problem, as we are lucky — and thankful — to have on-hand some of the most experienced and brilliant minds in the industry — our technical editors. So if your work "passes muster" and is published, you'll know you were reviewed by the best — and most demanding.

Chances are you'll be creating the paper under the auspices of the company for whom you work or own, or for one of the various industry-relevant associations. That means they as well will bask in the reflected glory that accrues with publication in *Power Transmission Engineering*.

For publication guidelines and more information, please contact Randy Stott at *stott@agma.org*

Power Transmission Engineering®

FREE SUBSCRIPTION

24PTEALL

☐ Renew my subscription ☐ NEW subscriber

☐ **YES** I want to receive/continue to receive ***PTE*** ☐ **NO**

Name ______________________________

Job Title ______________________________

Company Name ______________________________

Company Address ______________________________

City ______________________________

State ______________________________

Zip Code ______________________________

Signature: ______________________________ *(required)*

Date: ______________

Please send

☐ PRINT Version

☐ DIGITAL Version (E-mail required)

E-MAIL: ______________________________

☐ BOTH Print and Digital

*You can OPT OUT at any time.

How is THIS LOCATION involved with power transmission products?

(Check all that apply)

☐ WE **MAKE** power transmission products

☐ WE **BUY** power transmission products

☐ WE **SELL** power transmission products (distributors, sales reps, etc.)

☐ WE **DESIGN** products with power transmission components in them

☐ Other (please describe) ______________________________

What is your company's principal product or service?

____

Your mailing label on the cover looks like this:

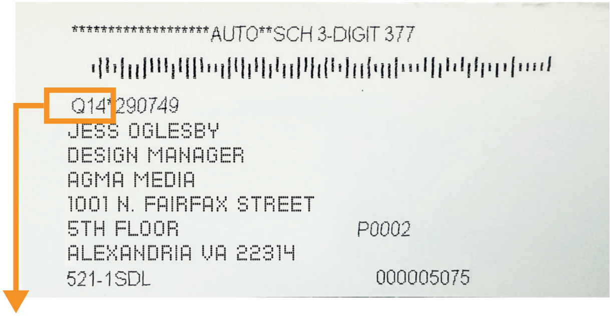

X/Y - means you have recieved a complimentary copy. Please complete this form to continue receiving your FREE copy of PTE.

Q14 (shown above) - means you have 14 issues remaining in your subscription (a NEW subscription has 16 issues).

Q1 - means you have 1 remaining issue before your PTE subscription expires. Please complete this form to renew.

MAIL to: 1001 N. Fairfax St, Suite 500, Alexandria, VA 22314 USA | **SCAN to:** *subscribe@powertransmission.com* | **FAX to:** 1.847.437.6618

Murder. Mayhem. Machine Shops.

Matthew Jaster, Senior Editor

Fear comes in many forms. Every October we exploit these fears—everything from spiders, zombies, and clowns to serial killers, puppets or twin girls standing in a hallway. A recent conversation with colleagues about Halloween attractions prompted a discussion on the role manufacturing/engineering plays in shocking the senses this time of year.

And believe me when I say that the "fear of manufacturing" is a real thing.

Exhibit number one is the Eastern State Penitentiary's Halloween Festival in Philadelphia.

"Hidden away from the world is a long-forgotten machine shop. Evil pervades this space—an evil with one mind but with many bodies. Will you survive or will you become just another cog in the machine?"

This is the premise for one of 13 Halloween attractions at the massive festival that contains five haunted houses, as well as historic tours, themed bars, live entertainment and more. Eastern State Penitentiary was once the most famous prison in the world, but stands today in ruin, a lost world of crumbling cellblocks and empty guard towers. This gothic structure, with soaring 30-foot-high fortress walls, is intimidating enough during the day. At night, the cellblocks fall into darkness and the penitentiary takes on a different energy.

Halloween Nights brings visitors into the penitentiary's cellblocks, exercise yards, workshops, outdoor courtyards, and hidden nooks. Nearly every inch of the penitentiary complex is activated for the event that takes place from late September to early November. The Machine Shop is just one of its shocking and alarming attractions where "visitors walk a one-way path and encounter menacing shop workers, eager for you to join their crew."

More worrisome is the popular feature to "opt in" for a more intense experience. If they choose, visitors can pick up a glow necklace at the entrance to the festival. Anyone wearing a glow necklace may be grabbed, sent into hidden passageways, and even temporarily separated from their group—all in the name of "Shocktober" thrills and chills.

It's really the machine shop noises—the cutting, grinding, drilling, the hand tools, the scraping of metal as you turn a corner that makes me think this is equal parts fantastic and alarming. This is why characters like Freddy Krueger, Leatherface and Jigsaw continue to influence today.

Each season the Eastern State Penitentiary adds new content to the festival. It will be interesting to hear what horrors the Machine Shop conjures up in 2025.

easternstate.org/

PTE

Editor's Note: Although Halloween has come and gone, the evil, dark shadow lord known as Mariah Carey will soon cover the world in her "All I Want for Christmas Is You," holiday sing-along. This diabolical earworm is significantly more terrifying than anything mentioned in this article—proceed through December with the upmost caution!